Updated: Feb 5, 2024

Costs of Generating Electrical Energy

1.0 Overview

The short-run costs of electrical energy generation can be divided into two broad areas: fixed and variable costs. These costs are illustrated in Fig. 1a below.

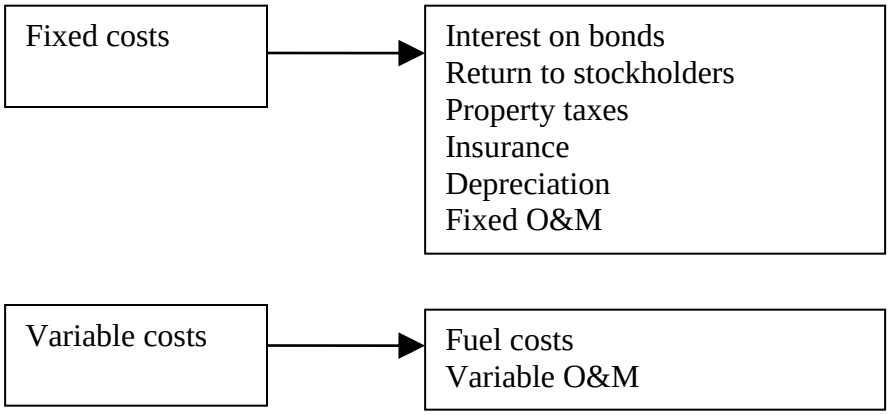

Fig. 1a

Typical values of these costs are given in the following Table 1 [1]. Some notes of interest follow:

- The "overnight cost" is the cost of constructing the plant, in $/kW if the plant could be constructed in a single day. However, values given here are out-of-date; better data is provided in the next set of notes.
- Operational values, including emissions rates, are ok.
  - The "variable O&M" is in mills/kWhr (a mill is 0.1¢). These values represent mainly maintenance costs. They do not include fuel costs.
  - Fuel costs are computed through the heat rate. We will discuss this calculation in depth.
  - The heat rate values given are average values.

Table 1

Technology	Size (MW)	Lead Time (Years)	Overnight Cost in 2009 (2008 US$/kW)	Variable O&M (2008 mills/kWh)	Fixed O&M (2008 US$/kW)	Heat Rate in 2009 (Btu/kWhr)	Emissions (lb/MWhr)				
							CO_2	SO_2	NO_x	Particulate	Hg
Scrubbed pulverized supercritical coal new	600	4	2,223	4.69	28.15	9,200	1,681	0.7007	0.579	0.107	9.45E-06
Integrated coal-gasification combined cycle (IGCC)	550	4	2,569	2.99	39.53	8,765	1,459	0.0942	0.406	0.053	4.24E-06
IGCC with carbon sequestration	380	4	3,776	4.54	47.15	10,781	154	0.0751	0.366	0.056	4.48E-06
Conventional gas/oil combined cycle	250	3	984	2.11	12.76	7,196	727.65	Negligible	0.203	Negligible	Negligible
Advanced gas/oil combined cycle	400	3	968	2.04	11.96	6,752	783	Negligible	0.06	Negligible	Negligible
Adv gas combined cycle with carbon sequestration	400	3	1,932	3.01	20.35	8,613	85.8	Negligible	0.066	Negligible	Negligible
Conventional combustion turbine	160	2	685	3.65	12.38	10,788	266.8	None	0.117	Negligible	None
Advanced combustion turbine	230	2	648	3.24	10.77	9,289	217.7	None	0.117	Negligible	None
Fuel cells	10	3	5,478	49.00	5.78	7,930	None	None	None	None	None
Advanced nuclear	1,350	6	3,820	0.51	92.04	10,488	None	None	None	None	None
Biomass	80	4	3,849	6.86	65.89	9,451	Negligible	0.07	1.575	0.27	Unknown
Geothermal	50	4	1,749	0.00	168.33	32,969	Negligible	Negligible	Unknown	Unknown	Unknown
Landfill gas	30	3	2,599	0.01	116.80	13,648	Unknown	Unknown	1.833	0.388	Unknown
Conventional hydropower	500	4	2,291	2.49	13.93	N/A	None	None	None	None	None
Wind	50	3	1,966	0.00	30.98	N/A	None	None	None	None	None
Wind offshore	100	4	3,937	0.00	86.92	N/A	None	None	None	None	None
Concentrated solar power	100	3	5,132	0.00	58.05	N/A	None	None	None	None	None
Photovoltaic	5	2	6,171	0.00	11.94	N/A	None	None	None	None	None

We focus on operating costs in these notes. Our goal is to characterize the relation between the cost and the amount of electric energy out of the power plant.

2.0 Fuels

Fuel costs dominate the operating costs necessary to produce electrical energy (MW) from the plant, sometimes called production costs. We begin with nuclear. Enriched uranium (3.5% U-235) in a light water reactor has an energy content of 960MWhr/kg [2], or multiplying by 3.41 MBTU/MWhr, we get 3274MBTU/kg. The total cost of bringing uranium to the fuel rods of a nuclear power plant, considering mining, transportation, conversion[1], enrichment, fabrication, and disposal was estimated to be (as of 12/2011) $2770/kg [3] ([4] gives a lower number as of 3/2017 to be $1390/kg). The two assessments, and more recent ones [5] are provided in the table below.

	Ref [3] Estimate		Ref [4] estimate 2020		Ref [5] estimate 2021		Ref [5] estimate 2023	
Uranium[2]	8.9 kg U_3O_8x$146	US$1300	8.9 kg U_3O_8x$68	$605	8.9 kg U_3O_8x$78.5	$698	8.9 kg U_3O_8x$78.5	$767
Conversion	7.5 kg U x $13	US$98	7.5 kg U x $14	$105	Avg of refs [3, 4]	$101.50	Avg of refs [3, 4]	$101.50
Enrichment[3]	7.3 SWU x $155	US$1132	7.3 SWU x $52	$380	7.3 SWU x $105.40	$769.42	7.3 SWU x $101.03	$738
FuelFabrication	per kg	US$240	per kg	$300	Avg of refs [3, 4]	$270	Avg of refs [3, 4]	$270
Total approx$/kg		2770		1390		1838		1876

[1] "Conversion" here does not mean to electric energy. Rather, uranium concentrates are purified and *converted* to uranium hexafluoride (UF6) or feed (F), the feed for uranium enrichment plants. See EPRI Rprt 1020659, "Parametric Study of Front-End Nuclear Fuel Cycle Costs Using Reprocessed Uranium," Jan. 2010.

[2] Uranium quantities are expressed in the unit of measure U3O8e (equivalent). U3O8e is triuranium octoxide (or uranium concentrate) and the equivalent uranium-component of uranium hexafluoride (UF6) and enriched uranium.

[3] Separative work unit (SWU): The standard measure of enrichment services. The effort expended in separating a mass F of feed of assay xf into a mass P of product assay xp and waste of mass W and assay xw is expressed in terms of the number of separative work units needed, given by the expression SWU = WV(xw) + PV(xp) - FV(xf), where V(x) is the value function, defined as V(x) = (1 - 2x) 1n((1 - x)/x).

Using the higher value of the above table, the cost per MBTU of nuclear fuel is about \$2770/kg ÷ 3274MBTU/kg =\$0.85/MBTU[4].

To give some idea of the difference between costs of different fossil fuels, some typical average costs of fuel are given in the Table 2 [6] for coal, petroleum, and natural gas. One should note in particular that

- The ratio of highest to lowest average price over the last 20-years for coal, petroleum, and natural gas are by factors of 1.9, 4.1, and 3.8, respectively, so coal has had more stable price variability than petroleum and natural gas.
- During 2022, coal is \$2.36/MBTU, petroleum \$16.53/MBTU, and natural gas \$7.21/MBTU, so coal is clearly a more economically attractive fuel for producing electricity (gas may look better than coal if a price for CO2 emissions is implemented).
- The 1992-2011 data of Table 2 was obtained from EIA sources that are no longer available; these data may not be highly accurate. The more recent data, 2012-2022, obtained from [7], should be OK.

[4] This is a very low fuel cost! However, it is balanced by a relatively high investment (overnight) cost – see Table 1.

Table 2: Receipts, Average Cost, and Quality of Fossil Fuels for the Electric Power Industry, 1991 through 2022

Table 4.5. Receipts, Average Cost, and Quality of Fossil Fuels for the Electric Power Industry, 1992 thru 2022

Year	Coal [1]				Petroleum [2]				Natural Gas [3]		All Fossil Fuels
	Receipts (Billion BTU)	Average Cost ($ per 10^6 Btu)	Average Cost (dollars/ ton)	Avg. Sulfur Percent by Weight	Receipts (billion BTU)	Average Cost ($ per 10^6 Btu)	Average Cost (dollars/ barrel)	Avg. Sulfur Percent by Weight	Receipts (Billion BTUs)	Average Cost ($/ 10^6 Btu)	Average Cost $/$10^6$ Btu)
1992		1.41	29.36	1.29						2.32	1.5
1993		1.38	28.58	1.18						2.56	1.59
1994		1.35	28.03	1.17						2.23	1.52
1995	16,946,807	1.32	27.01	1.08	532,564	2.68	16.93	0.9	3,081,506	1.98	1.45
1996	17,707,127	1.29	26.45	1.10	673,845	3.16	19.95	1	2,649,028	2.64	1.52
1997	18,095,870	1.27	26.16	1.11	748,634	2.88	18.3	1.1	2,817,639	2.76	1.52
1998	19,036,478	1.25	25.64	1.06	1,048,098	2.14	13.55	1.1	2,985,866	2.38	1.44
1999	18,460,617	1.22	24.72	1.01	833,706	2.53	16.03	1.1	2,862,084	2.57	1.44
2000	15,987,811	1.2	24.28	0.93	633,609	4.45	28.24	1	2,681,659	4.3	1.74
2001	15,285,607	1.23	24.68	0.89	726,135	3.92	24.86	1.1	2,209,089	4.49	1.73
2002	17,981,987	1.25	25.52	0.94	623,354	3.87	24.45	0.9	5,749,844	3.56	1.86
2003	19,989,772	1.28	26.00	0.97	980,983	4.94	31.02	0.83	5,663,023	5.39	2.28
2004	20,188,633	1.36	27.42	0.97	958,046	5	31.58	0.88	5,890,750	5.96	2.48
2005	20,647,307	1.54	31.20[l]	0.98	986,258	7.59	47.61	0.77	6,356,868	8.21	3.25
2006	21,735,101	1.69	34.09	0.97	406,869	8.68	54.35	0.73	6,855,680	6.94	3.02
2007	21,152,358	1.77	35.48	0.96	375,260	9.59	59.93	0.71	7,396,233	7.11	3.23
2008	21,280,258	2.07	41.14	0.97	375,684	15.52	95.38	0.61	8,089,467	9.01	4.12
2009	19,437,966	2.22	44.47	0.99	330,043	10.44	64.18	0.51	8,319,329	5.50	3.04
2010	19,289,661	2.27	45.33	1.14	275,058	13.94	85.07	0.48	8,867,396	5.43	3.26
2011	18,675,843	2.40	47.67	1.16	216,752	20.30	122.72	0.53	9,250,652	5.00	3.29
2012		2.38	46.09	1.25		12.48	73.30	3.61		3.42	2.83
2013		2.34	45.33	1.29		11.57	68.09	3.54		4.33	3.09
2014		2.37	45.96	1.34		11.60	68.12	3.56		5.00	3.31
2015		2.22	42.86	1.38		6.74	39.51	3.38		3.23	2.65
2016		2.11	40.64	1.34		5.24	30.46	3.69		2.87	2.47
2017		2.06	39.27	1.28		7.10	41.23	3.59		3.37	2.65
2018		2.06	39.25	1.31		9.68	56.82	3.31		3.55	2.83
2019		2.02	38.70	1.31		9.07	53.55	3.03		2.88	2.5
2020		1.92	36.36	1.28		5.98	34.92	3.45		2.40	2.22
2021		1.98	37.48	1.30		10.08	58.93	3.11		5.20	3.82
2022		2.36	44.69	1.28		16.53	97.42	2.91		7.21	5.22
2023											

[1] Anthracite, bituminous coal, subbituminous coal, lignite, waste coal, and synthetic coal.

[2] Distillate fuel oil (all diesel and No. 1, No. 2, and No. 4 fuel oils), residual fuel oil (No. 5 and No. 6 fuel oils and bunker C fuel oil), jet fuel, kerosene, petroleum coke (converted to liquid petroleum, see Technical Notes for conversion methodology), and waste oil.

[3] Natural gas, including a small amount of supplemental gaseous fuels that cannot be identified separately. Natural gas values for 2001 forward do not include blast furnace gas or other gas.

[4] Beginning in 2002, data from the Form EIA-423, "Monthly Cost and Quality of Fuels for Electric Plants Report" for independent power producers and combined heat and power producers are included in this data dissemination. Prior to 2002, these data were not collected; the data for 2001 and previous years include only data collected from electric utilities via the FERC Form 423.

[5] For 2003 only, estimates were developed for missing or incomplete data from some facilities reporting on the FERC Form 423. This was not done for earlier years. Therefore, 2003 data cannot be directly compared to previous years' data. Additional information regarding the estimation procedures that were used is provided in the Technical Notes.

R = Revised.

Notes: Totals may not equal sum of components because of independent rounding. Receipts data for regulated utilities are compiled by EIA from data collected by the Federal Energy Regulatory Commission (FERC) on the FERC Form 423. These data are collected by FERC for regulatory rather than statistical and publication purposes. The FERC Form 423 data published by EIA have been reviewed for consistency between volumes and prices and for their consistency over time. Nonutility data include fuel delivered to electric generating plants with a total fossil-fueled nameplate generating capacity of 50 or more megawatts; utility data include fuel delivered to plants whose total fossil-fueled steam turbine electric generating capacity and/or combined-cycle (gas turbine with associated steam turbine) generating capacity is 50 or more megawatts. Mcf = thousand cubic feet. Monetary values are expressed in nominal terms.

Sources: Energy Information Administration, Form EIA-423, "Monthly Cost and Quality of Fuels for Electric Plants Report;" Federal Energy Regulatory Commission, FERC Form 423, "Monthly Report of Cost and Quality of Fuels for Electric Plants."

Check www.eia.gov/electricity/monthly/ for the most recent month's data on this.

2.0 Natural gas

One obvious indication from the Table 2 data is that the price of natural gas has been reducing. We can see this another way from Figure 1b below.

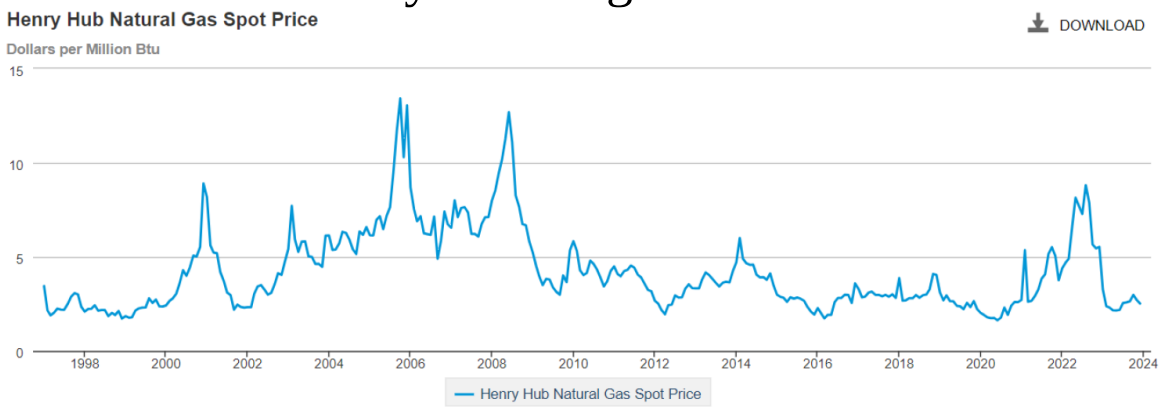

Figure 1b: Price of natural gas, 1997-2024

But even with high gas prices, as seen in 2000-2009 period, especially relative to the price of coal (less than $2.00/MBTU for most of this period) the 2000-2009 period saw new combined cycle gas-fired plants far outpace new coal-fired plants, with gas accounting for over 85% of new capacity [8] (of the remaining, 14% was wind). The reasons for this was that gas-fired combined cycle plants have (i) low capital costs, (ii) high fuel efficiency, (iii) short construction lead times, and (iv) low emissions.

This trend has been ongoing for some time, as observed in Fig. 2a [9], where the sharply rising curve from 1990-2022 is due to gas consumption for electric. In addition to the previous (i)-(iv) reasons, there are two more: (v) low gas prices (due to shale), and (vi) the need for power system flexibility (due to wind and solar growth).

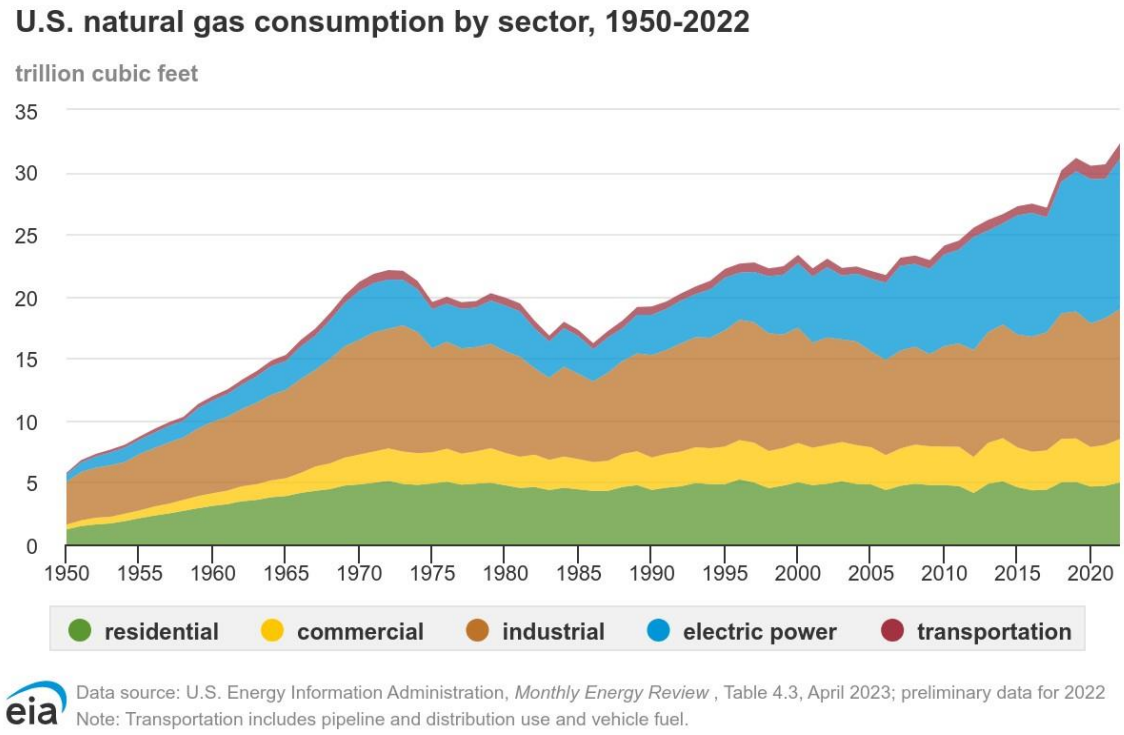

Fig. 2a: US Natural Gas Consumption 1950-2022

This view of natural gas can be also observed in Table 3a, where one sees that in the last row, the sum of coal+gas+wind remains about constant, showing that energy reduction from coal has been mainly compensated by energy increases in gas and wind.

Table 3a: Electric energy production by resource type

	2000	2008	2010	2015	2016	2018	2019	2021	2022
FOSSIL									
OIL	1.9%	1.6%	1.0%	0.8%	0.7%	0.7	0.5%	0.5%	0.5%
COAL	57%	49%	45%	33%	30%	27%	23.4%	21.9%	19.7%
NAT GAS	10%	20%	23%	33%	34%	34%	38.4%	38.4%	39.9%
OTHER GAS		0.4%		0.5%	0.5%	0.5%	0.3%	0.3%	0.3%
NUCLEAR	23%	19.4%	20%	20%	20%	19%	19.7%	18.9%	18.2%
RNWBLES									
HYDRO	7.5%	7%	7%	6%	6%	6.8%	6.7%	6.0%	6.0%
WIND	0%	0.6%	1.8%	4.7%	5.6%	8.3%	7.3%	9.2%	10.3%
SOLAR	0%	0.1%	0.1%	0.6%	0.9%	1.5%	2.6%	2.8%	3.4%
BIOMASS	0.2%	1.3%	1.5%	1.6%	1.6%	1.7%	1.4%	1.3%	1.2%
GEOTRML	0.4%	0.4%	0.4%	0.4%	0.4%	0.4%	0.4%	0.4%	0.4%
Coal+gas+wind	67%	69.4%	69.8%	70.7%	69.6%	69.3%	69.1%	69.5%	69.9%

Today's very low natural gas prices are due to the increased supply from shale gas, which has always been in the ground but not economically attractive to get until hydraulic fracturing was developed. Fig. 3a illustrates hydraulic fracturing, where water and sand are injected into the ground at very high pressures to force out the gas that resides within shale fissures.

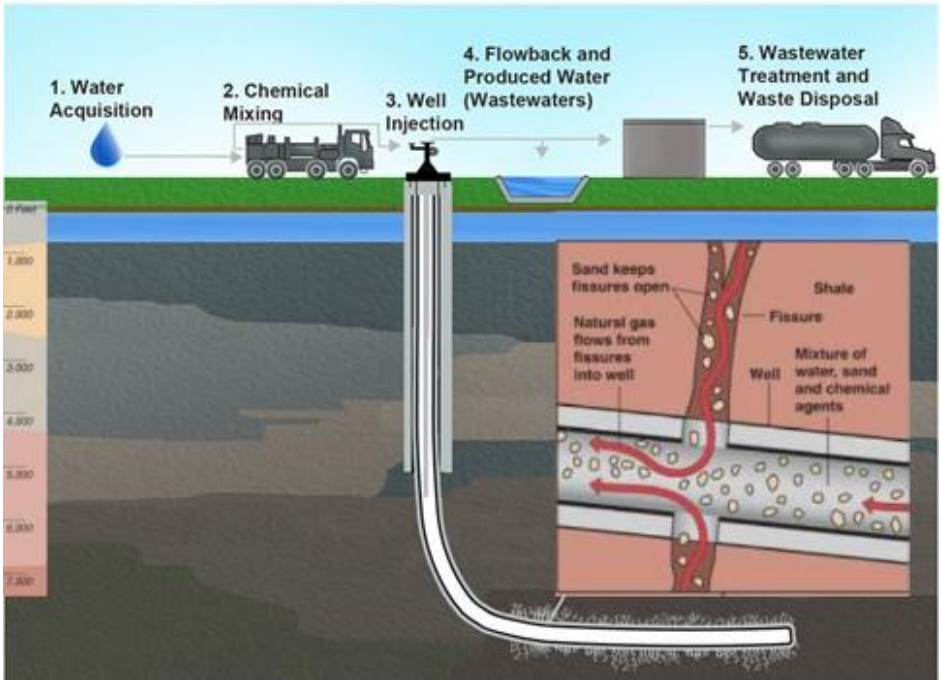

Figure 3a: Hydraulic fracturing

Although the Marcellus shale play has been the most productive in recent years, there are others, per Fig. 3b.

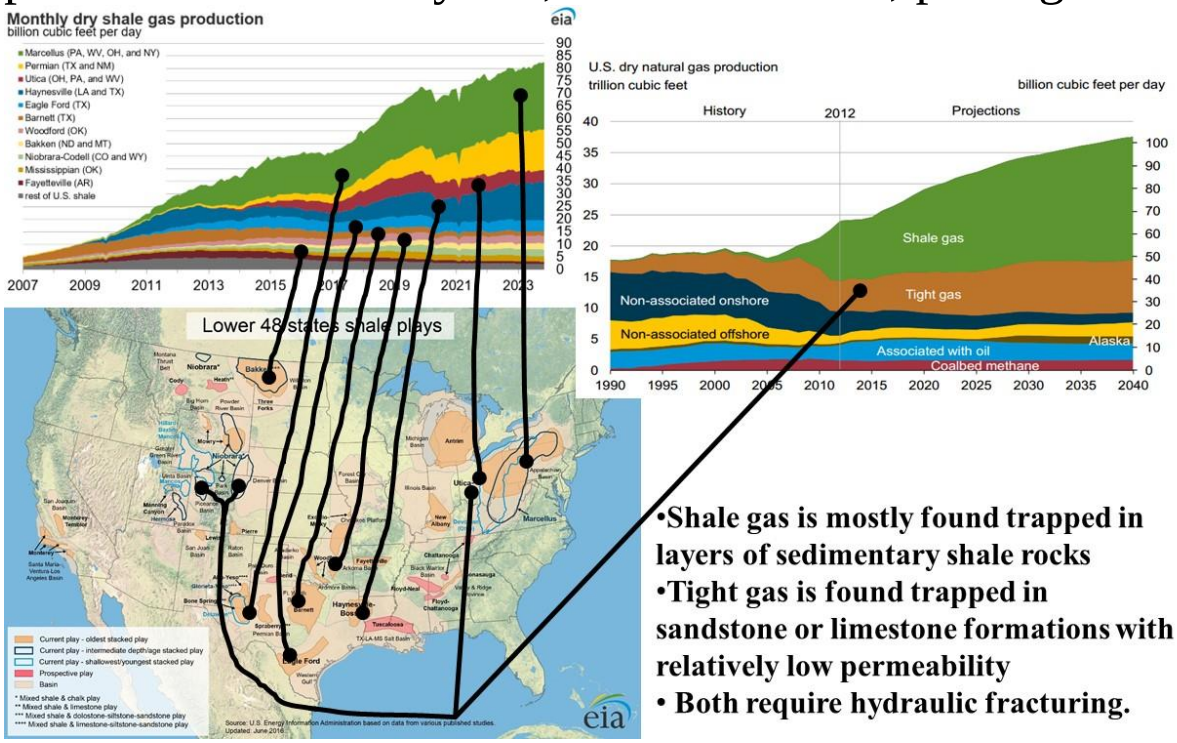

•Shale gas is mostly found trapped in layers of sedimentary shale rocks
•Tight gas is found trapped in sandstone or limestone formations with relatively low permeability
• Both require hydraulic fracturing.

Fig. 3b: US shale plays

Fig. 3c [10][5] shows the preponderance of natural gas-fueled power plants in the Eastern Interconnection, particularly in the northeast. It is also apparent that California uses a great deal of natural gas-fueled power plants (California uses no coal for power gen).

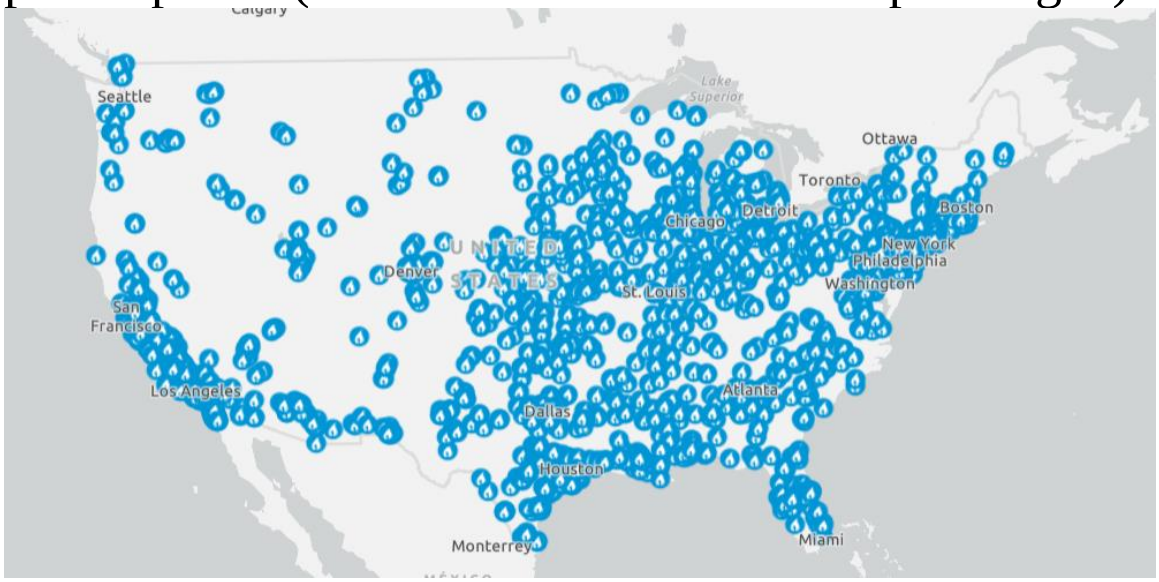

Fig. 3c: Gas power plants in the US

Fig. 3d compares US average gas flows in 2005 (before much shale gas production) to those of 2014 (when shale gas production was fairly high). The black curve is an important interface that shows gas flowing *into* the northeast in 2005 and *out of* the northeast in 2014 (mainly due to the Marcellus play).

[5] One should note reference [10]; this is a very versatile electric energy infrastructure mapping tool.

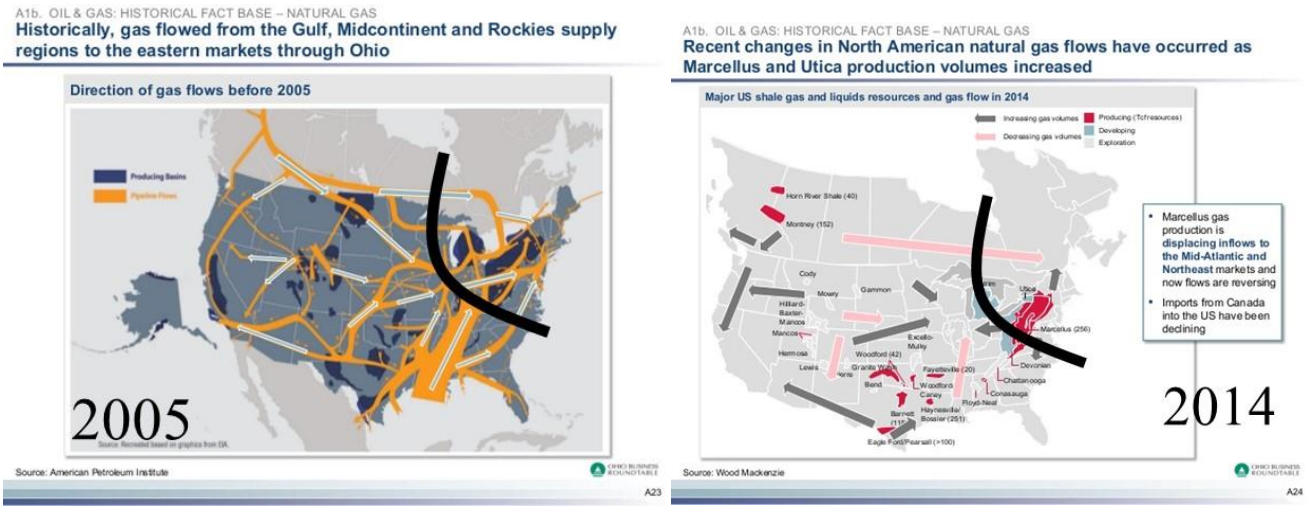

Fig. 3d

Fig. 4 shows the (i) reduction in Gulf of Mexico gas production, (ii) reduction in Canadian imports, and increase in Pennsylvania gas production (mainly from the Marcellus play).

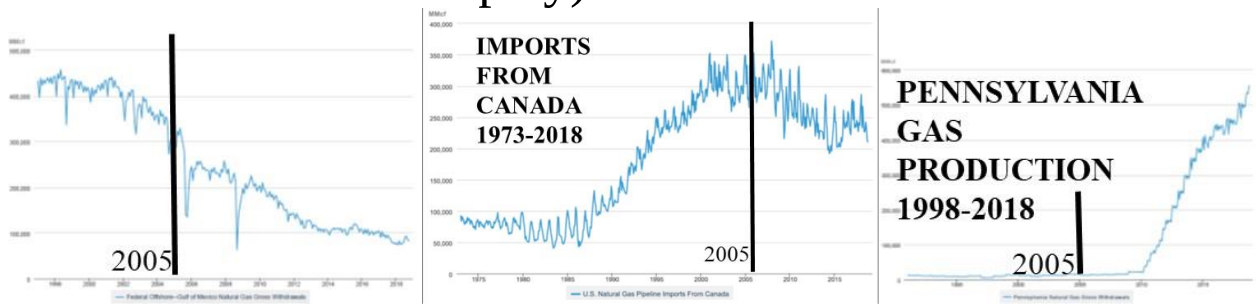

Fig. 4: Changes in main gas production resources due to Shale

Over the last five years, most new US generating capacity has been natural gas, wind, or solar, as indicated in Fig. 5a [11] and Fig. 5b [12].

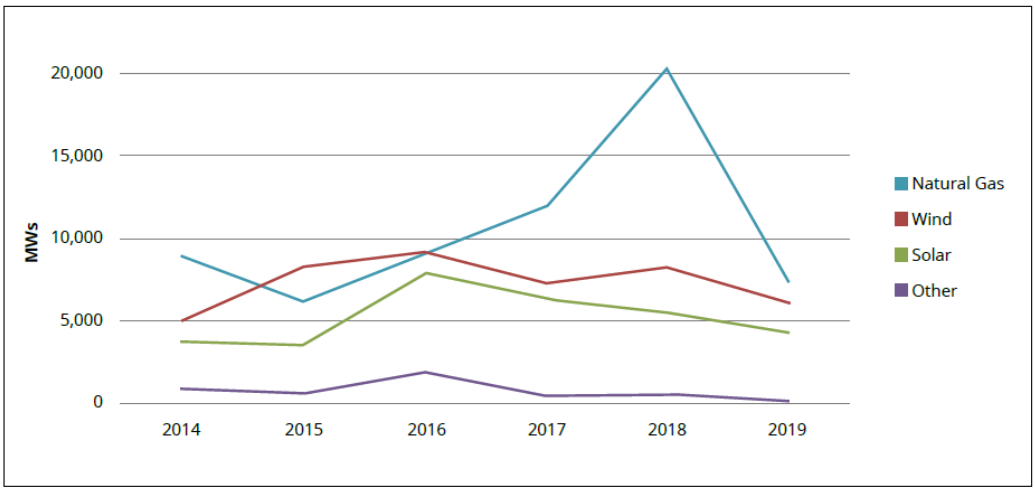

Fig. 5a: Capacity additions MW by yr: 2014-‘19 [11]

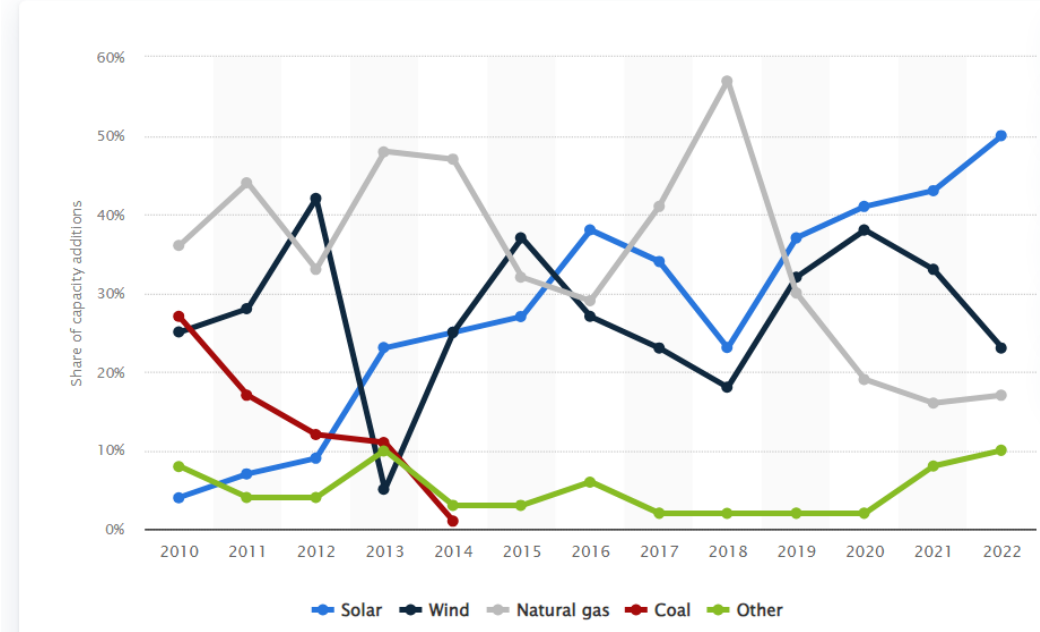

Fig. 5b: Capacity additions % by yr: 2010-2022 [12]

Planned capacity will likely continue to emphasize gas, solar, and wind plants, as indicated in Fig. 5c [13]. These plots, developed in 2020, reflect predicted cumulative capacity in each year. The plot on the upper left is for “Tier 1 planned capacity” which might be considered to be ***very*** *likely to be built*. The plot on the upper right is for “Tier 1 & Tier

2 planned capacity," where Tier 2 might be considered to be *likely to be built* [6] [7]. The plot on the lower middle, developed 2023, is for "Tier 1 & Tier 2 planned capacity" and gives the same information as the plot in the upper right, except 2 years later [14].

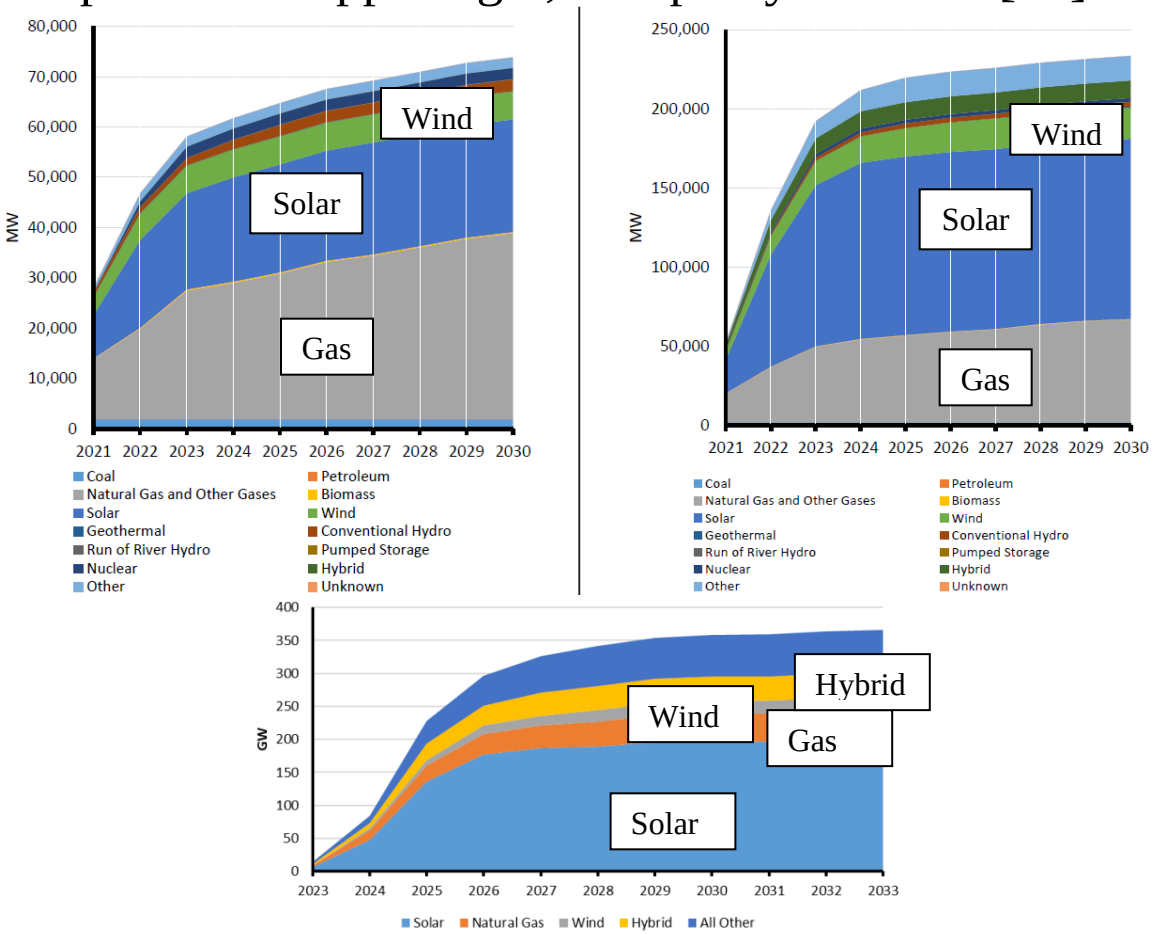

Fig. 5c: 10-year projection of US capacity additions [13]

[6] Tier 1: Planned capacity that meets at least one of the following requirements are included as anticipated resources: • Construction complete (not in commercial operation) • Under construction • Signed/approved Interconnection service agreement • Signed/approved power purchase agreement • Signed/approved Interconnection construction service agreement • Signed/approved wholesale market participant agreement • Included in an integrated resource plan or under a regulatory environment that mandates a resource adequacy requirement (applies to vertically integrated entities).

[7] Tier 2: Planned capacity that meets at least one of the following requirements are included as prospective resources: • Signed/approved completion of a feasibility study • Signed/approved completion of a system impact study • Signed/approved completion of a facilities study • Requested Interconnection service agreement • Included in an integrated resource plan or under a regulatory environment that mandates a resource adequacy requirement (applies to regional transmission organizations (RTOs)/independent system operators (ISOs)).

3.0 Fuels continued – transportation & emissions

For electric systems, the ways of moving bulk quantities of energy in the nation are via rail & barge (for coal), gas pipeline, & electric transmission, illustrated in Fig. 6a.

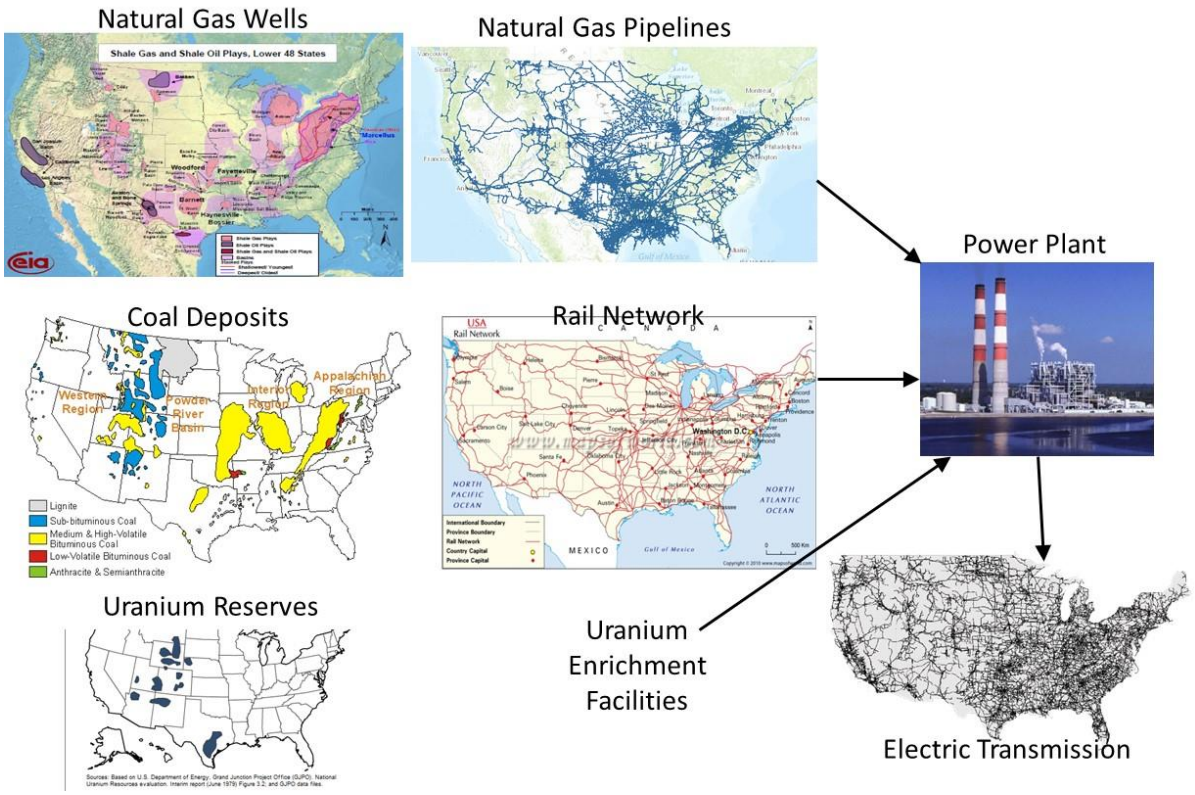

Fig. 6a

An important influence in the way fuel is moved is restrictions on sulfur dioxide (SO2) due to the highly successful cap and trade program started in 1995.

Coal is classified into 4 ranks: lignite (Texas, N. Dakota), sub-bituminous (Wyoming), bituminous (central Appalachian), anthracite (Penn), reflecting the progressive increase in age, carbon content, & heating value per unit weight. Fig. 6b shows US coal resources [15].

Fig. 6b: US coal resources [15]

Table 3b illustrates differences in coal throughout the US in capacity, heat-value, sulfur content, & mine-mouth price. These data are accurate, with exception of minemouth price. Appalachian coal is mainly bituminous, mainly mined underground, whereas Wy. coal is subbituminous, mainly surface-mined.

Table 3b: Coal characteristics from different US locations

	Supply node	Productive capacity (thousand short tons)	Avg. heat value (MMBtu/ton)	Avg. sulfur content (lbs. sulfur/MMBtu)	Avg. minemouth price (2002 $/short ton)
Anthracite	Northern Appalachia	169,819	24.04	1.83	24.79
Bituminous	Central Appalachia	335,926	25.03	0.75	30.18
	Southern Appalachia	28,221	24.66	0.57	33.61
	Illinois Basin	121,801	22.73	2.03	22.86
	Western Interior	2,538	23.58	2.28	27.86
Lignite	Gulf Coast Lignite	56,063	13.10	1.62	17.02
	North Dakota Lignite	32,400	13.24	1.15	8.46
Subbituminous	Powder River Basin	479,761	17.45	0.39	6.63
	Rocky Mountains	75,185	22.81	0.40	17.96
	Southwest	56,653	20.22	0.63	22.47
	Northwest	7,284	15.63	1.13	8.92

Although Table 3b is a little dated (2002), its general message that Wyoming coal (Powder River Basin, PRB) is our most important source is still relevant, as confirmed by Fig. 7a below [16], where we see PRB coal production being over twice that of the next highest source; this is due to (a) its $/BTU is very attractive, and (b) it has low sulfur content. As a result, a great deal of coal is transported from Wyoming eastward, as illustrated in Fig. 7a (the right-hand-side of Fig. 7 is an eastbound coal train through Ames, Iowa).

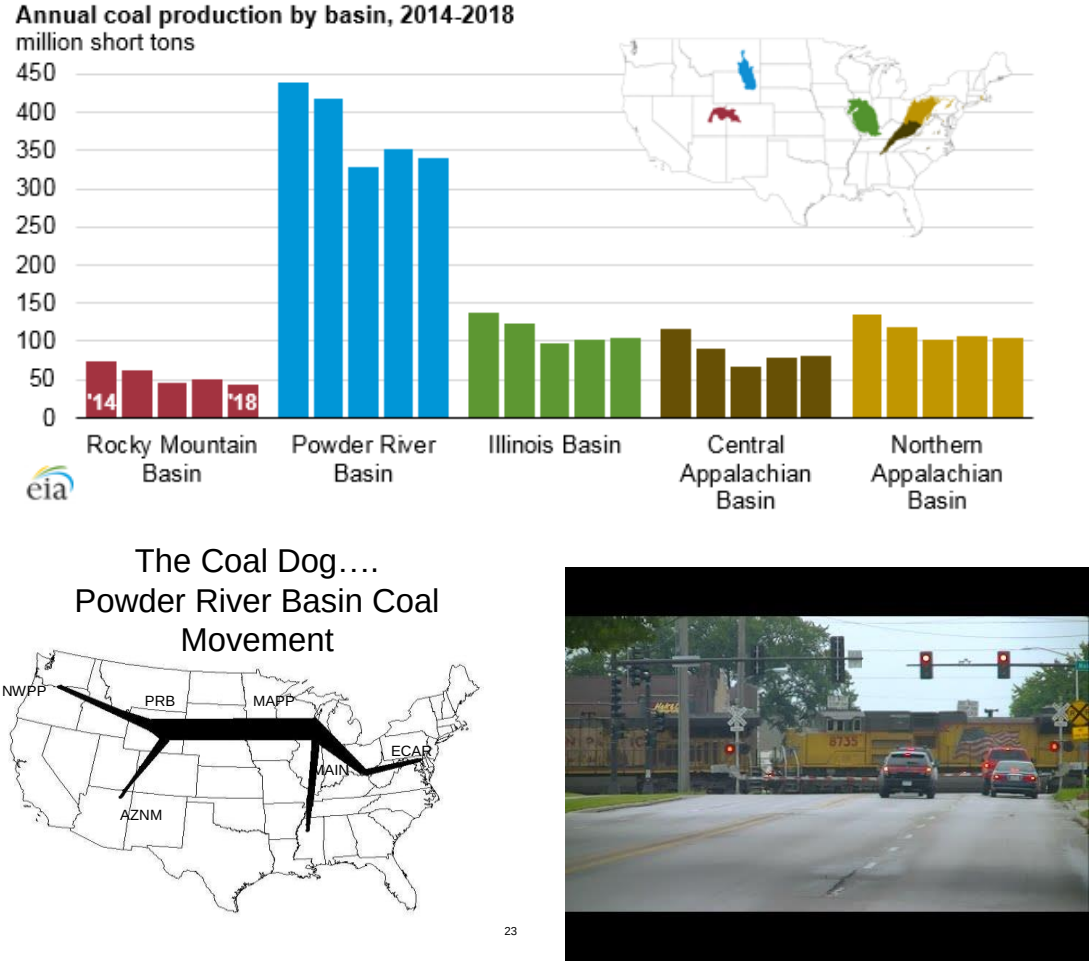

Fig. 7a: PRB coal movement

We do not have a national CO_2 market yet, but there is a regional one called the Regional Greenhouse Gas Initiative (RGGI) that involves 11 eastern states [17]. The essence of RGGI is shown in Fig. 7b [18].

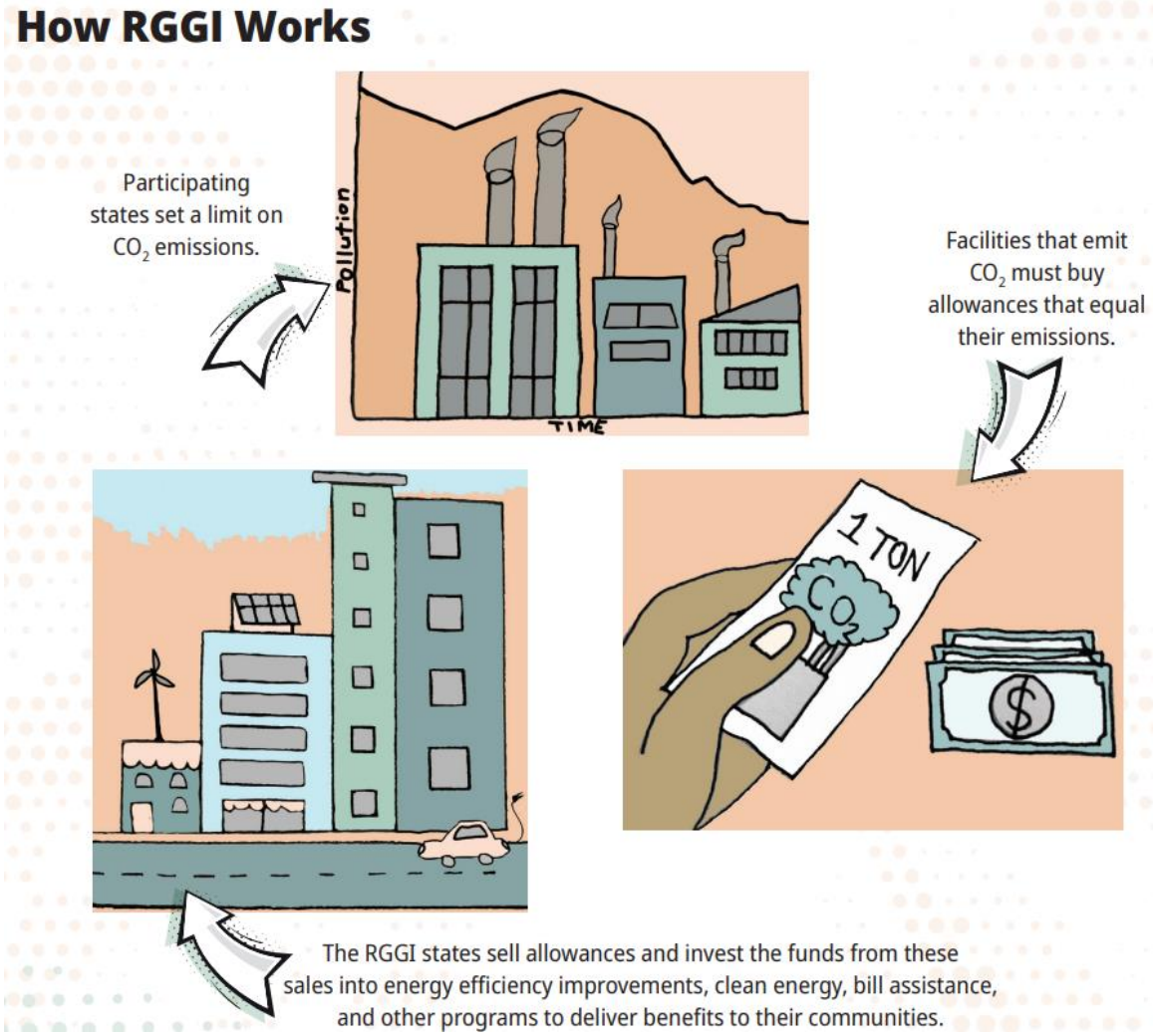

Fig. 7b: How RGGI works [18]

4.0 CO_2 Emissions - overview

There is increased acceptance worldwide that global warming is caused by emission of greenhouse gasses into the atmosphere. These greenhouse gases are (in order of their contribution to the greenhouse effect on Earth) [19]:

- Water vapor: causes 36-70% of the effect
- Carbon dioxide (CO_2): causes 9-26% of the effect
- Methane (CH_4): causes 4-9% of the effect
- Nitrous oxide (N_2O):
- Ozone (O_3): causes 3-7% of the effect
- Chlorofluorocarbons (CFCs) are compounds containing chlorine, fluorine, and carbon, (no H_2). CFCs are commonly used as refrigerants (e.g., Freon).

The DOE EIA was publishing an excellent annual report on annual US greenhouse gas emissions; the one published in Nov, 2007 (for 2006) is [20], and the one published in Dec, 2009 (for 2008) is [21]. One figure from the 2006 report is provided as Fig. 8a. The information of most interest to us in Fig. 8a is the center, summarized in Table 4.

Note each greenhouse gas is quantified by "million metric tons of carbon dioxide equivalents," or $MMTCO_2e$. Carbon dioxide equivalents are the amount of CO_2 by weight emitted into the atmosphere that would produce the same estimated radiative forcing as a given weight of another radiatively active gas [20].

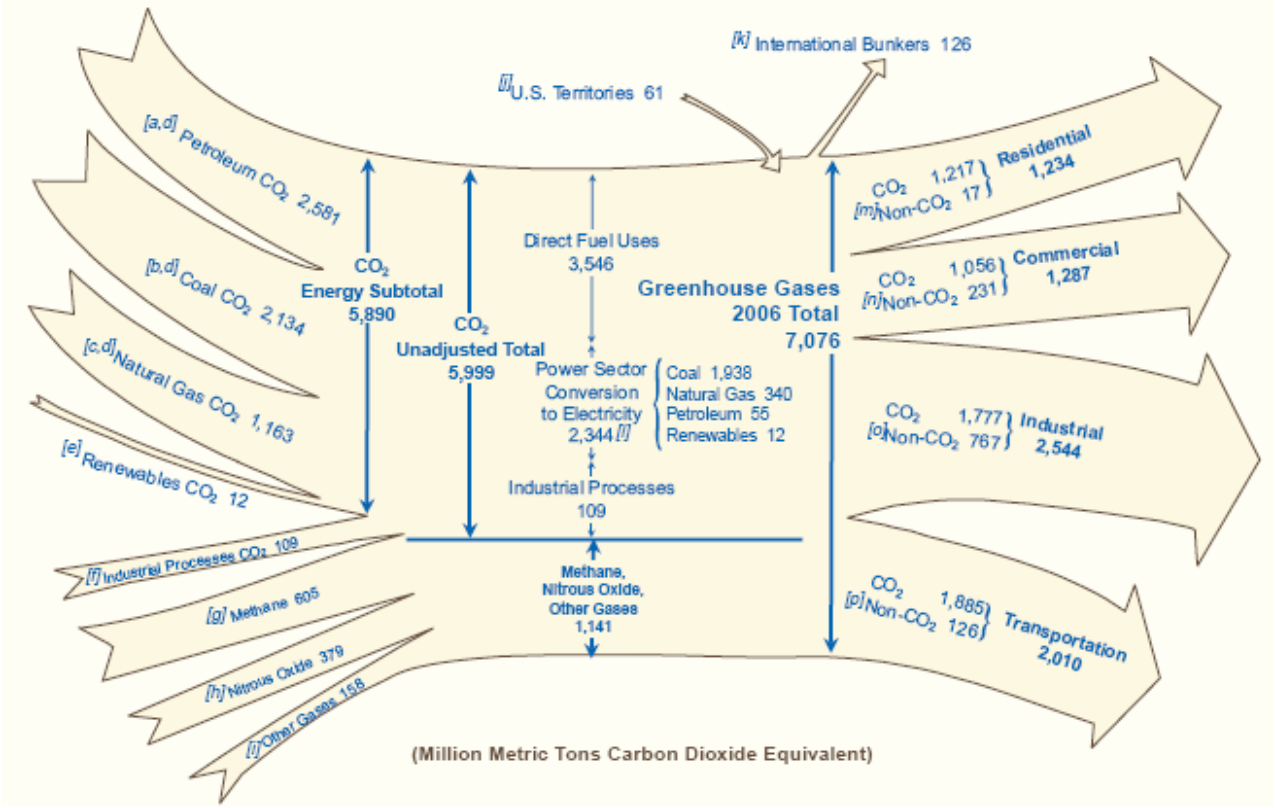

Fig. 8a: Summary of US Greenhouse Gas Emissions, 2006

Table 4: Greenhouse Gas Total, 2006

Sectors	MMTCO_2e	% total CO_2	% total GHG
From Power Sector	2344	39.1	32.8**
*From DFU-transp	1885	31.4	26.4**
*From DFU-other	1661	27.7	23.3**
From ind. processes	109	1.8	1.5**
Total CO_2	5999	100	84.0
Non-CO_2 GHG	1141		16.0
Total GHG	7140		100.

*The direct fuel use (DFU) sector includes transportation, industrial process heat, space heating, and cooking fueled by petroleum, natural gas, or coal. The DFU-transportation CO_2 emissions of 1885 MMT was obtained from the lower right-hand-side of Fig. 9a. The DFU-other CO_2 emissions of 1661 MMT was obtained as the difference between total DFU emissions of 3546 MMT (given at top-middle of Fig. 9a) and the DFU-transportation emissions of 1885 MMT.

** The "% total GHG" for the 4 sectors (power, DFU-transp, DFU-other, and ind processes) do not include the Non-CO_2 GHG emitted from these four sectors, which are lumped into the single row "Non-CO2 GHG." If we assume that each sector emits the same percentage of Non-CO2 GHG as CO_2, then the numbers under "% total CO_2" are representative of each sector's aggregate contribution to CO_2 emissions. The only sector we can check this for is transportation, where we know Non-CO_2 emissions are 126MMT, which is only 11% of the 1141 MMT total non-CO_2, significantly less than the % of total CO_2 for transportation, which is 31.4%.

Figure 8b [21] is the same picture as Fig. 8a except it is for the year 2008; the information is summarized in Table 5.

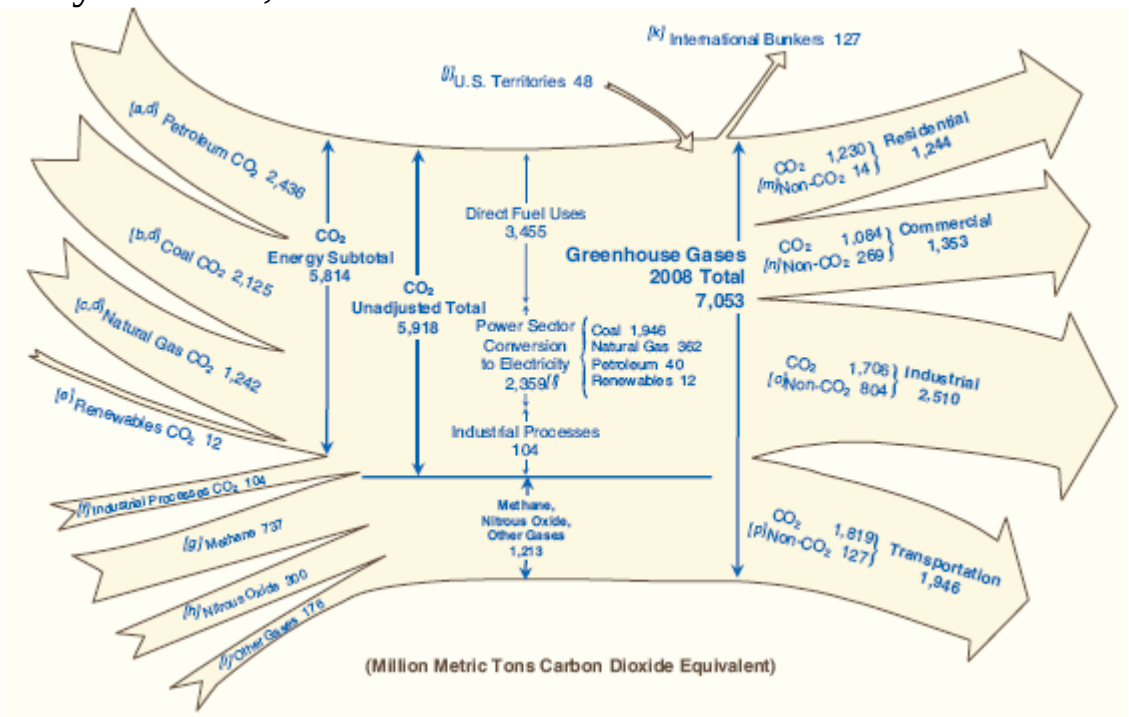

Fig. 8b: Summary of US Greenhouse Gas Emissions, 2008

Table 5: Greenhouse Gas Total, 2008

Sectors	MMTCO_2e	% total CO_2	% total GHG
From Power Sector	2359	39.8	33.18**
*From DFU-transp	1819	30.8	25.5**
*From DFU-other	1636	27.6	22.9**
From ind. processes	104	1.8	1.5**
Total CO_2	5918	100	83.0
Non-CO_2 GHG	1213		17.0
Total GHG	7131		100.

*The direct fuel use (DFU) sector includes transportation, industrial process heat, space heating, and cooking fueled by petroleum, natural gas, or coal. The DFU-transportation CO_2 emissions of 1819 MMT was obtained from the lower right-hand-side of Fig. 9b. The DFU-other CO_2 emissions of 1636 MMT was obtained as the difference between total DFU emissions of 3555 MMT (given at top-middle of Fig. 9b) and the DFU-transportation emissions of 1819 MMT.

** The "% total GHG" for the 4 sectors (power, DFU-transp, DFU-other, and ind processes) do not include the Non-CO_2 GHG emitted from these four sectors, which are lumped into the single row "Non-CO2 GHG." If we assume that each sector emits the same percentage of Non-CO2 GHG as CO_2, then the numbers under "% total CO_2" are representative of each sector's aggregate contribution to CO_2 emissions. The only sector we can check this for is transportation, where we know Non-CO_2 emissions are 127MMT, which is only 10.5% of the 1213 MMT total non-CO_2, significantly less than the % of total CO_2 for transportation, which is 30.8%.

To check the above, I have provided the "emission flow" diagram from the Lawrence Livermore National Laboratory (LLNL) website [22], below, comparing its values with those of the 2008 EIA data, see Table 6. The significant takeaways are that (i) the LLNL diagram does not report non-CO_2 GHG; (ii) otherwise, the numbers agree very well.

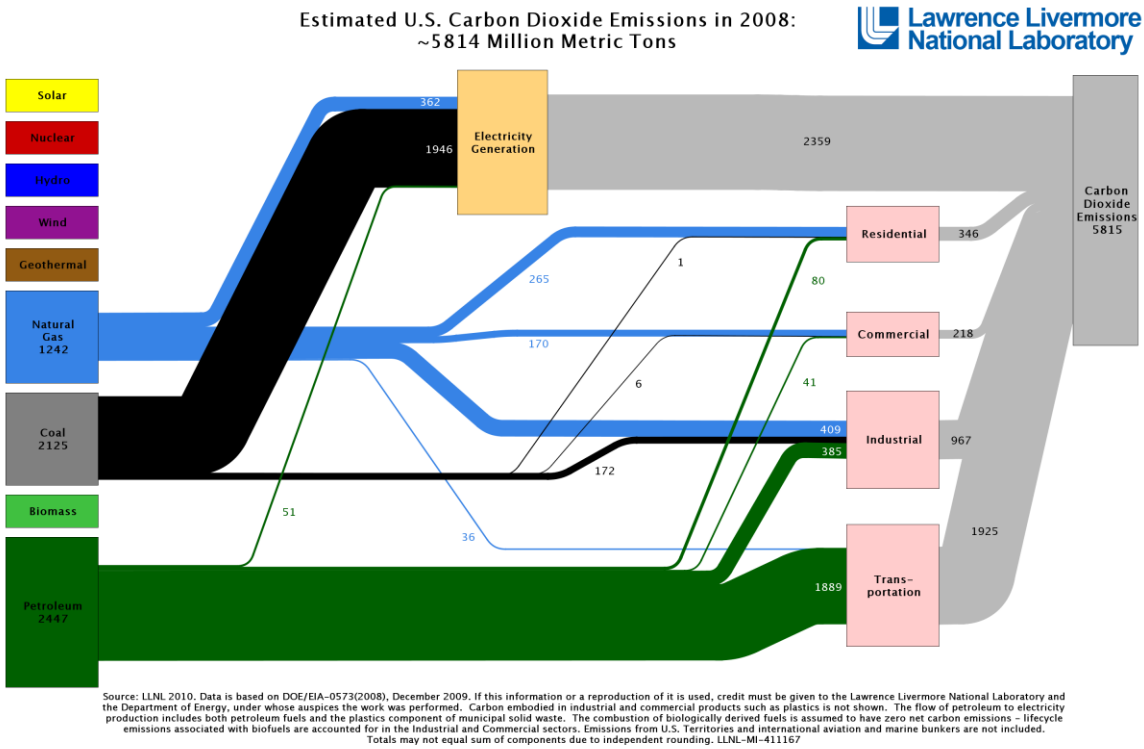

Fig. 9a: LLNL Emissions flow diagram for 2008

Table 6: CO_2 Emissions, 2008, comparing Fig. 8b data (first number in each cell) and Fig. 9a data (second number in each cell)

Sectors	$MMTCO_2e$	% total CO_2	% total GHG
From Power Sector	2359, 2359	39.8, 40.6	33.18**, NA
*From DFU-transp	1819, 1889	30.8, 32.5	25.5**, NA
*From DFU-other	1636, 1567	27.6, 26.9	22.9**, NA
From ind. processes	104, 0	1.8, 0	1.5**, NA
Total CO_2	5918, 5815	100, 100	83.0, NA
Non-CO_2 GHG	1213, Unreported		17.0, NA
Total GHG	7131, NA		100.

We now examine more recent emissions data from LLNL. Fig. 9a shows the LLNL emissions flow diagram for 2018, and Fig. 9b shows the one for 2022.

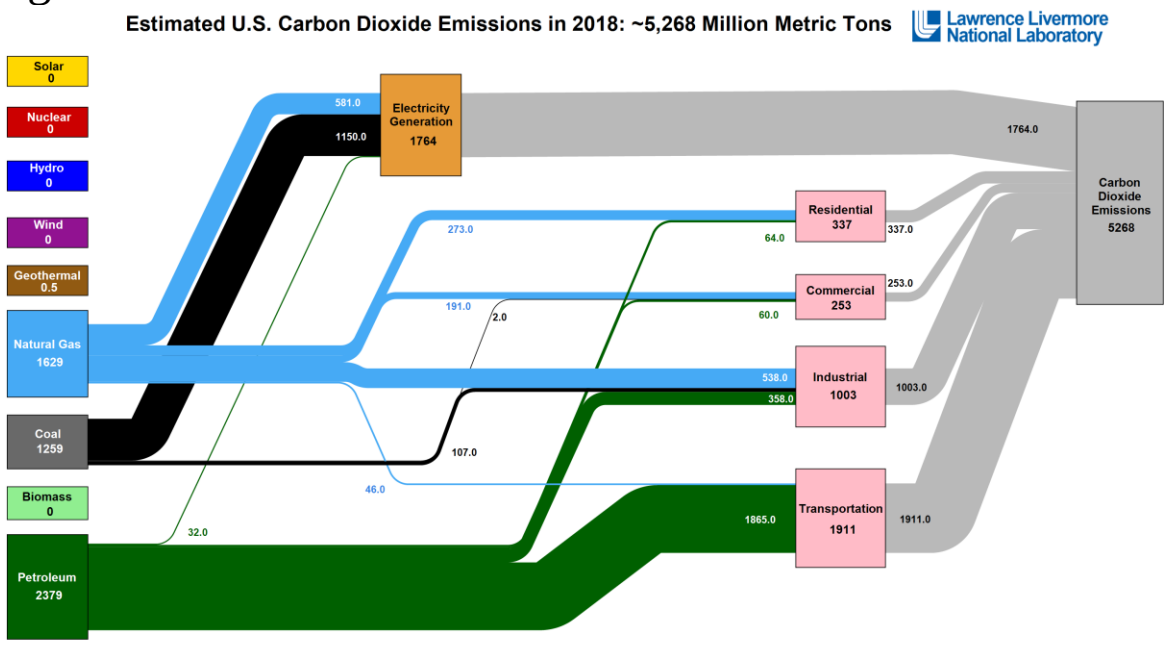

Source: LLNL July, 2019. Data is based on DOE/EIA MER (2018). If this information or a reproduction of it is used, credit must be given to the Lawrence Livermore National Laboratory and the Department of Energy, under whose auspices the work was performed. Carbon emissions are attributed to their physical source, and are not allocated to end use for electricity consumption in the residential, commercial, industrial and transportation sectors. Petroleum consumption in the electric power sector includes the non-renewable portion of municipal solid waste. Combustion of biologically derived fuels is assumed to have zero net carbon emissions – the lifecycle emissions associated with producing biofuels are included in commercial and industrial emissions. Totals may not equal sum of components due to independent rounding errors. LLNL-MI-410527

Fig. 9a: Summary of US Greenhouse Gas Emissions, 2018

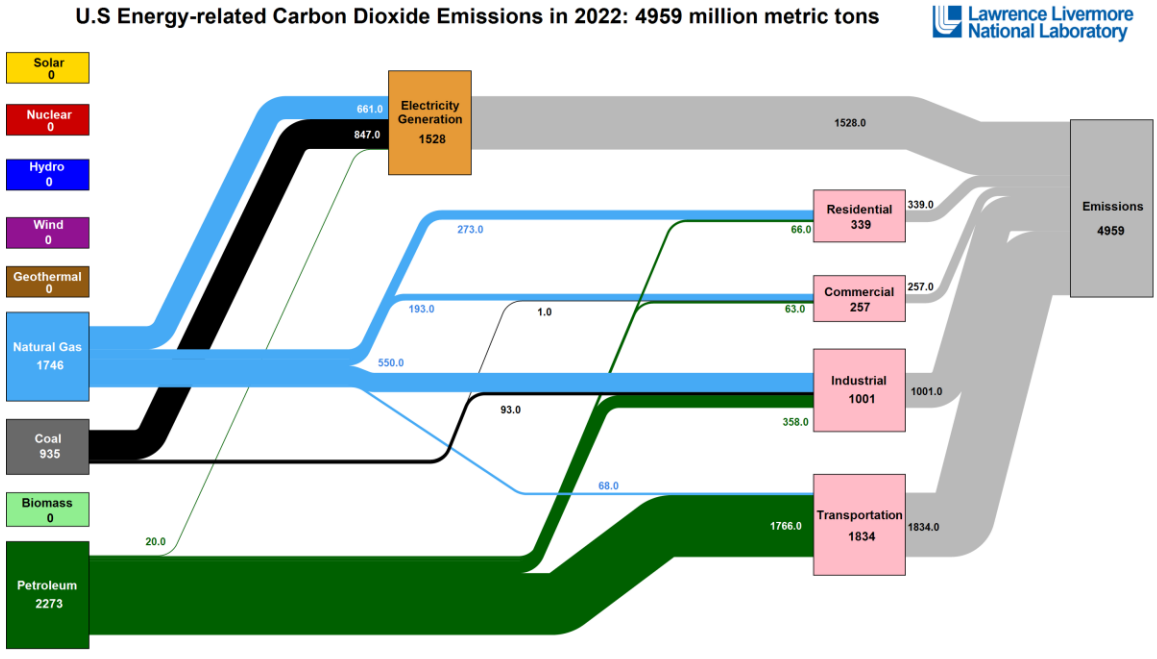

Source: LLNL July, 2023. Data is based on DOE/EIA Energy-Related CO2 Emissions (2022). If this information or a reproduction of it is used, credit must be given to the Lawrence Livermore National Laboratory and the Department of Energy, under whose auspices the work was performed. Carbon dioxide emissions are attributed to their physical source, and emissions from electricity production are not allocated to end use for electricity consumption in the residential, commercial, industrial, and transportation sectors. Petroleum consumption in the electric power sector includes the non-renewable portion of municipal solid waste. Combustion of biologically derived fuels is assumed to have zero net carbon emissions and The lifecycle emissions associated with producing biofuels are included in the commercial and industrial sectors. Totals may not equal sum of components due to independent Rounding. LLNL-MI-410527

Fig. 9b: Summary of US Greenhouse Gas Emissions, 2022

Some significant facts to remember from Table 6 are

- Total US CO_2 emissions have decreased from about 5800 MMT/yr in 2008 to 5268MMT/yr in 2018 to 4959/yr in 2022.
- In 2008, there were an additional 1200 MMT/yr CO_2 equivalents from other GHG.
- Percentage of CO_2 emissions from power sector is 40% in 2008, 33% in 2018, and 31% in 2022.
- Percentage of CO_2 emissions from transportation sector is 31% in 2008, 36% in 2018, & 37% in 2022.
- Percentage of CO_2 emissions from "other" is 27% in 2008, 30% in 2018, and 32% in 2022.

➔Most 2008-'22 CO_2 reduction has occurred in the power sector.

5.0 CO_2 Emissions – power sector

The left-hand plot of Figure 10 [23] shows that US CO_2 emissions from both the electric power and the transportation sectors were rising from 1988 to 2008, after which they both dipped significantly (due to the 2008 economic recession). However, the power sector continued to decline whereas the transportation sector began rising again. The right-hand plot of Fig. 10 shows that the dip in power sector emissions was characterized by a reduction in carbon intensity (amount of CO_2 produced per unit energy).

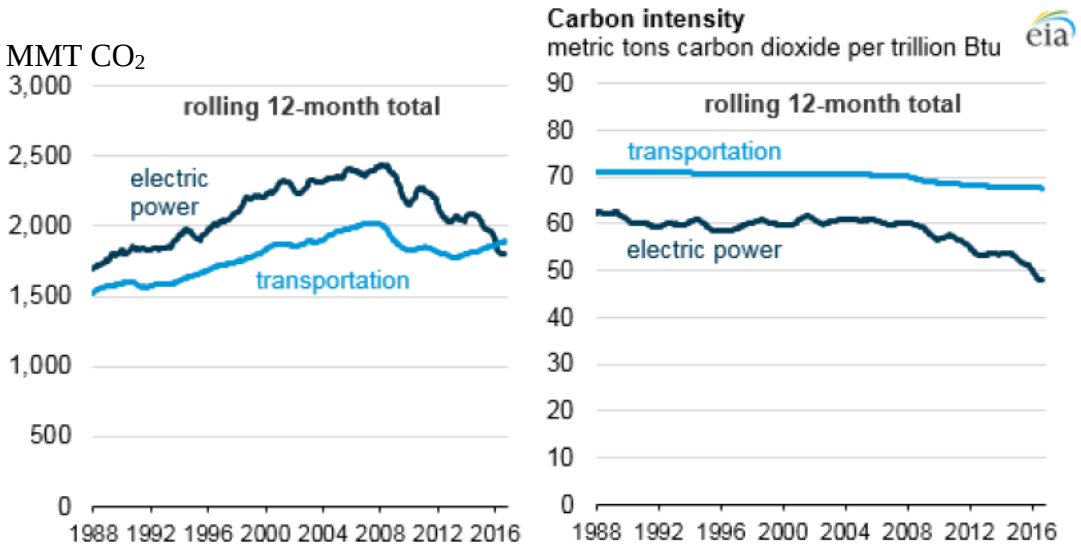

Fig. 10: Power/transportation CO_2 emissions & intensity by yr [23]

The reduction in electric power sector carbon intensity observed in the right-hand plot of Fig. 10 is an indication that the technologies used to produce electric energy are changing. This is confirmed by Fig. 11a [24] where we observe that coal and petroleum generation are being replaced by gas-fueled and "non-carbon" generation (which includes nuclear, hydro, wind, and solar). This conclusion is also confirmed in Fig. 11b [25], where we observe non-CO_2 sources shift from 28% in 2005 to 38% in 2017.

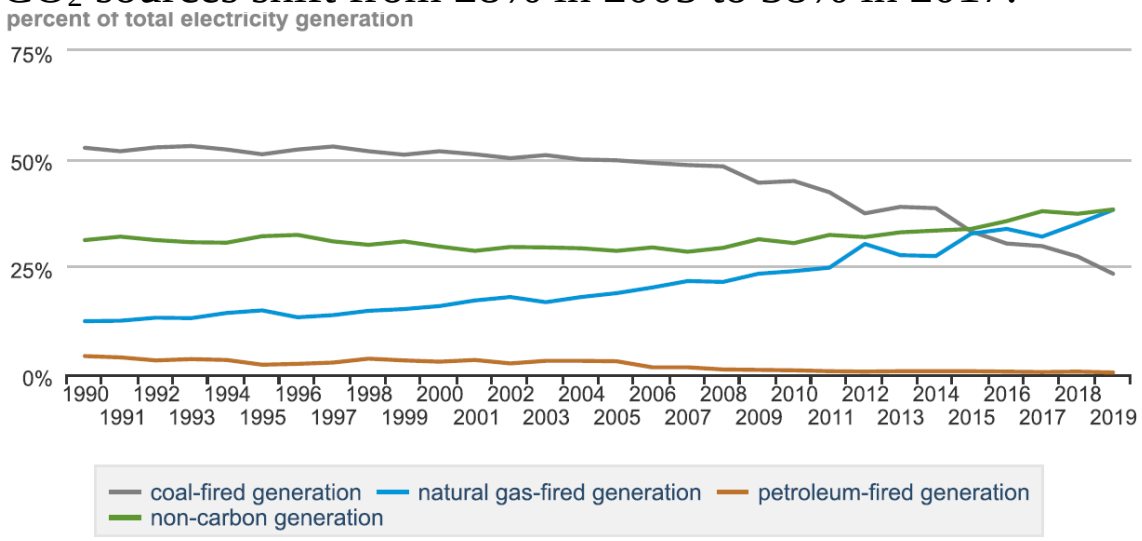

Fig. 11a: Percent of total generation for four types [24]

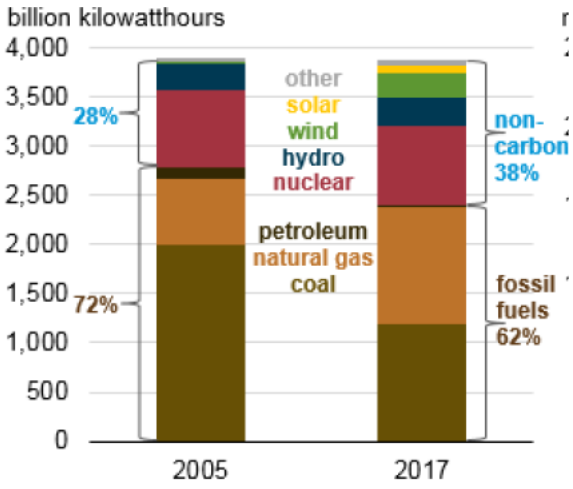

Fig. 11b: Percent of total gen for CO_2 vs non-CO_2 sources [25]

Fig. 11c [25] indicates that coal has been and remains the largest contributor to power sector CO_2 emissions. However, whereas it was responsible for about 1950MMT in 2007 (about 83%), it was responsible for only about 1250MMT in 2017 (about 73%). In these years, the next highest contributor was natural gas, at about 350 MMT in 2007 (15%) to about 450MMT in 2017 (26%). The two combined account for 98% of power sector CO_2 emissions in 2007 and 99% in 2017; from 2017 forward, petroleum is not a significant power sector CO_2 emitter.

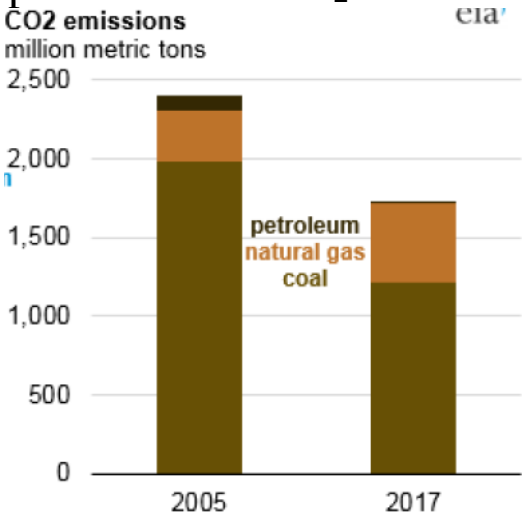

Fig. 11c: Power sector emissions from each fossil fuel type [25]

Fig. 11d [26] shows the US electric sector CO_2 emissions for gas-fueled generation and for coal-fueled generation. Here, it is observed that emissions from gas-fueled electric generation will soon exceed emissions from coal-fueled generation, an observation resulting from the increase in gas-fueled generation and retirements of coal-fueled generation.

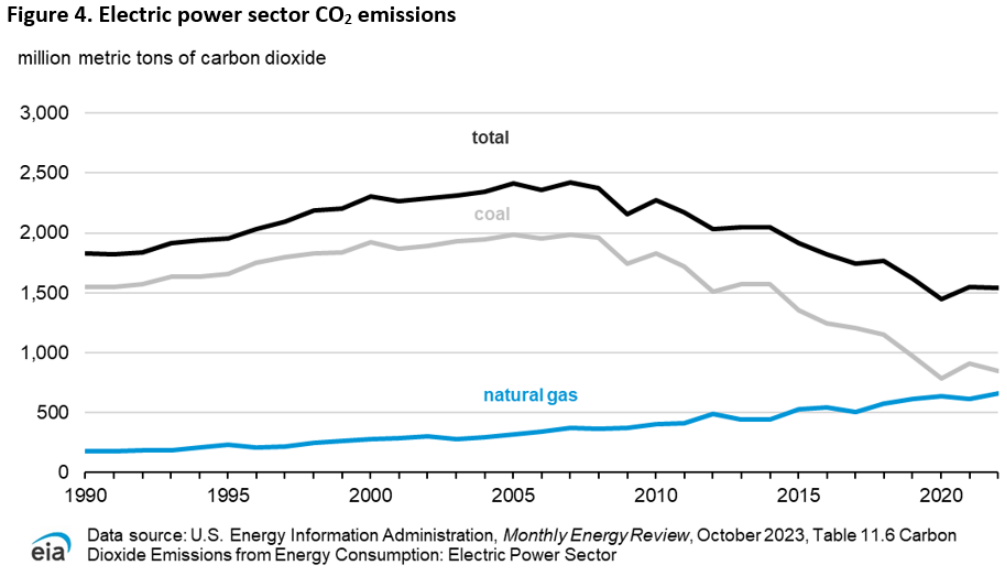

Fig. 11d: Electric power sector emissions for gas and coal [26]

The annual emissions from each fossil fuel is a function of
(a) how many MWhrs are produced from it;
(b) its ratio of CO_2 per unit energy content;
(c) its conversion efficiency.
We already discussed the influence of (a) (see Figs. 11a, 11b). We examine the influence of (b), (c) in Tables 7, 8.

The ratio of CO_2 per unit energy content is given in Table 7 below, in the last column, titled "pounds CO_2 per Million BTU." Here we observe that the fuels with highest CO_2 per unit energy content are, in decreasing order:

- Anthracite, 227
- Petroleum coke, 225
- Lignite, 215.4
- Subbituminous, 212.7
- Bituminous, 205.3
- Municipal solid waste 2, 199.85
- Wood and waste II, 195.0
- Tires/tire-derived fuel, 189.5
- Residual fuel (No 5 and no 6 fuel oil), 173.9
- Other petroleum fuels, 139-161
- Natural gas and other gaseous fuels, 115-139
- Renewables and nuclear, 0

Table 7: Emission Coefficients for Different Fuels

Fuel	Code	Emission Coefficients		
		Pounds CO2 per Unit Volume or Mass		Pounds CO2 per Million Btu
Petroleum Products				
Aviation Gasoline	AV	18.355	per gallon	152.717
Distillate Fuel (No. 1, No. 2, No. 4 Fuel Oil and Diesel)	DF	22.384	per gallon	161.386
Jet Fuel	JF	21.095	per gallon	156.258
Kerosene	KS	21.537	per gallon	159.535
Liquified Petroleum Gases (LPG)	LG	12.805	per gallon	139.039
Motor Gasoline	MG	19.564	per gallon	156.425
Petroleum Coke	PC	32.397	per gallon	225.13
Residual Fuel (No. 5 and No. 6 Fuel Oil)	RF	26.033	per gallon	173.906
Natural Gas and Other Gaseous Fuels				
Methane	ME	116.376	per 1000 ft3	115.258
Landfill Gas	LF	1	per 1000 ft3	115.258
Flare Gas	FG	133.759	per 1000 ft3	120.721
Natural Gas (Pipeline)	NG	120.593	per 1000 ft3	117.08
Propane	PR	12.669	per gallon	139.178
Coal	CL			
Anthracite	AC	5685	per short ton	227.4
Bituminous	BC	4931.3	per short ton	205.3
Subbituminous	SB	3715.9	per short ton	212.7
Lignite	LC	2791.6	per short ton	215.4
Renewable Sources				
Biomass	BM	Varies depending on the composition of the biomass		
Geothermal Energy	GE	0		0
Wind	WN	0		0
Photovoltaic and Solar Thermal	PV	0		0
Hydropower	HY	0		0
Tires/Tire-Derived Fuel	TF	6160	per short ton	189.538
Wood and Wood Waste 2	WW	3812	per short ton	195
Municipal Solid Waste 2	MS	1999	per short ton	199.854
Nuclear	NU	0		0

But CO_2 per unit energy content only characterizes the fuel; we also must consider the efficiency of the technologies using the fuel in order to obtain the CO_2/MWhr. To get this, we need efficiencies of the generation technologies. Fig. 12a provides such efficiencies; the resource from which it came [27] provides a good overview of various factors affecting generation efficiencies.

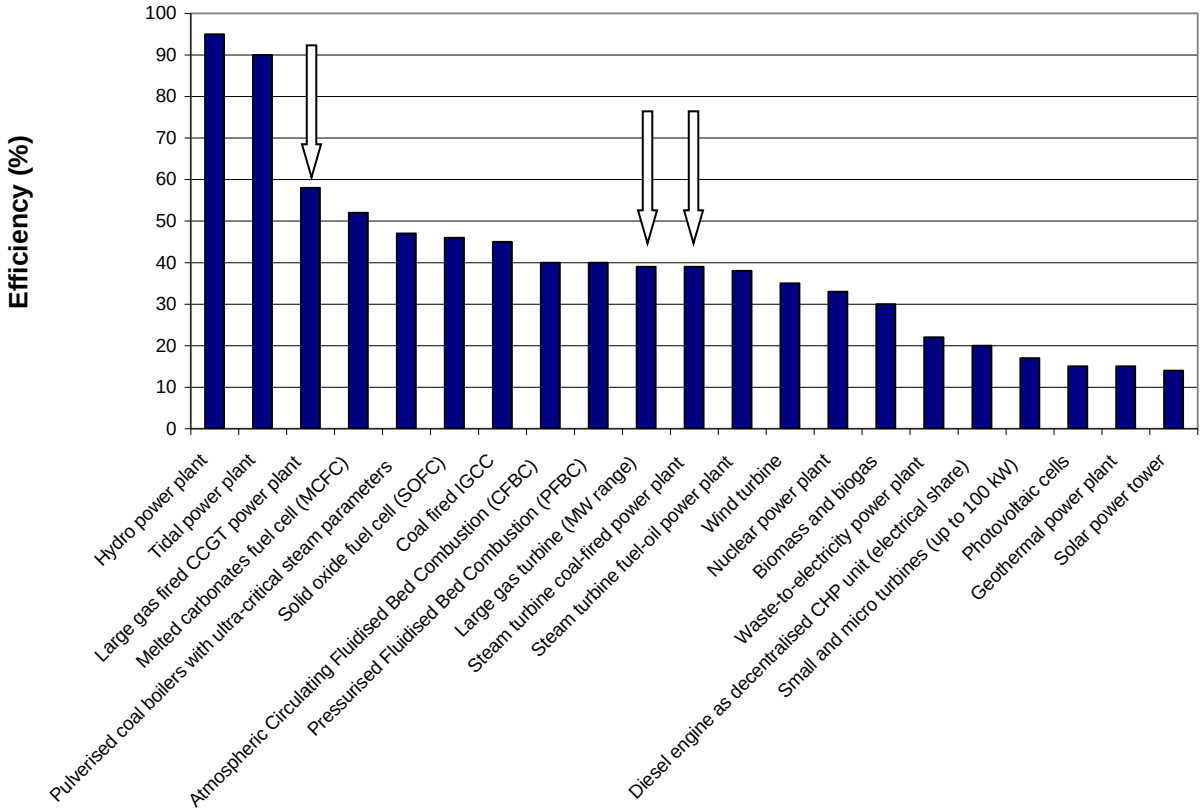

Fig. 12a: Generation efficiencies

Table 7 and Fig. 12a provide data to compare different technologies in terms of CO_2/MWhr. For example, let's compare a natural gas combined cycle (NGCC) plant (η=.58), a gas turbine (η=.39), and a coal-fired power plant (η=.39), where CO_2 content of natural gas is 117.08 lbs/MBTU and CO_2 content of coal (assuming it uses sub-bituminous) is 212.7 lbs/MBTU. (Note that as observed in Table 7, coal has different CO_2 per unit energy content, depending on type, as shown below [28]).

Table 8.6. Carbon Dioxide Emission Factors in EPA Base Case 2000

Fuel	Carbon Dioxide (lbs/mmBtu)
Bituminous Coal	205.3
Subbituminous Coal	212.7
Lignite	215.4

NGCC: $117.08\frac{lbs}{MBTU_{IN}} \times \frac{1MBTU_{IN}}{.58MBTU_{OUT}} \times \frac{3.41MBTU}{MWhr} = 688.5lbs/MWhr$

Gas turbine:

$$117.08\frac{lbs}{MBTU_{IN}} \times \frac{1MBTU_{IN}}{.39MBTU_{OUT}} \times \frac{3.41MBTU}{MWhr} = 1023.7lbs/MWhr$$

Coal-fired plant:

$$212.7\frac{lbs}{MBTU_{IN}} \times \frac{1MBTU_{IN}}{.39MBTU_{OUT}} \times \frac{3.41MBTU}{MWhr} = 1859.8lbs/MWhr$$

The gas turbine emits 55% of what the coal plant emits, although they have same efficiency (due to lower CO_2 per unit energy content). With the more efficient NGCC plant, we obtain emissions of only 37% of the coal plant.

Table 8 [29] indicates a pulverized coal (PC) plant, a circulating fluidized bed (CFB) plant, and an integrated gasification combined cycle (IGCC) plant all have emissions/MWhr rates similar to the coal plant assessed above. The combined cycle plant (an NGCC) has a bit higher ratio (810 instead of 688.5) because it used a lower efficiency (49.3% instead of 58%).

Table 8: Typical technology emission coefficients

Constituent	Unit	PC	CFB	IGCC	Combined Cycle
Fuel		Coal	Coal	Coal	Natural Gas
NO_x	lb/MBtu	0.05 - 0.07	0.07 – 0.11	0.055 – 0.10	0.007-0.013
	lb/MWh	0.55	0.85	0.68	0.07
SO_2	lb/MBtu	0.06 – 0.1	0.04 – 0.13	0.015 – 0.045	0.0006
	lb/MWh	0.74	0.80	0.27	0.004
PM/PM_{10} (filterable)	lb/MBtu	0.012 – 0.015	0.012 – 0.015	0.005 – 0.01	~ 0.020 – 0.025
	lb/MWh	0.12	0.13	0.07	0.15
CO_2	lb/MBtu	205-220	205-220	205-220	117
	lb/MWh	1950	1990	1910	810

Notes:
Mercury regulation has recently been vacated. New permitting efforts will proceed on a case-by-case basis.
Air emissions based on 100 percent load.
CO2 emissions are not currently regulated.
IGCC is without CO_2 capture and storage.

In the calculations at the top of the previous page, one can recognize that the 3.41/η factor in each equation is just the unit heat rate in MBTU/MWhr. This means the same calculation can be done by multiplying the lbs/$MBTU_{IN}$ factor from Table 7 by the average heat rate for the plant.

We can also convert the above to Metric tons/MWhr by dividing by 2204 lbs/Metric ton, to get the following figures:

Wind and solar:	0 MT/MWhr
NGCC:	0.312 MT/MWhr
Gas turbine:	0.464 MT/MWhr
Coal-fired plant:	0.844 MT/MWhr.

It is interesting to compare these values with emission coefficients given by region/state [30]. A sample of some of these coefficients are provided below for 2002, '15, '22.

State	2002 MT/mwh
Vermont	0.013
Washington	0.111
California	0.275
New York	0.389
Penn	0.574
Georgia	0.619
Texas	0.664
Ohio	0.817
Iowa	0.854
Kentucky	0.911
N Dakota	1.017
US Avg	0.606

State	2015 MT/mwh
Vermont	0.028
Washington	0.085
California	0.205
New York	0.211
Penn	0.388
Iowa	0.453
Georgia	0.454
Texas	0.476
Ohio	0.665
N Dakota	0.755
Kentucky	0.887
US Avg	0.453

State	2022 MT/mw
Vermont	0.00045
Washington	0.08394
California	0.16878
New York	0.21597
Penn	0.30989
Iowa	0.28766
Georgia	0.31897
Texas	0.36298
Ohio	0.50998
N. Dakota	0.60708
Kentucky	0.7863
US Avg.	0.36479

Why is Iowa so high in 2002?
What happened in Iowa from 2002-2022?
Why are N.Dakota & Kentucky so high in 2002?
What happened in N. Dakota from 2002-2022?
Why is California so low in all three years?
Why is Washington so low in all three years?
Why is Vermont so low in all three years?
What happened to Vermont from 2002-2022?
Why did US avg decrease 2002-2022?

Iowa was, in 2002, heavily dependent on coal. Today, with Iowa's wind growth, it is less so, but still, coal is still a large part of Iowa's generation portfolio – see Fig. 12b [31, 32], where one notes generation from wind surpassed generation from coal in ~2020. In 2022, Iowa's coal and

wind gen % were 25 & 63, respectively [33]. As of 8/2020, Iowa has no nuclear (Duane Arnold plant closed 8/2020).

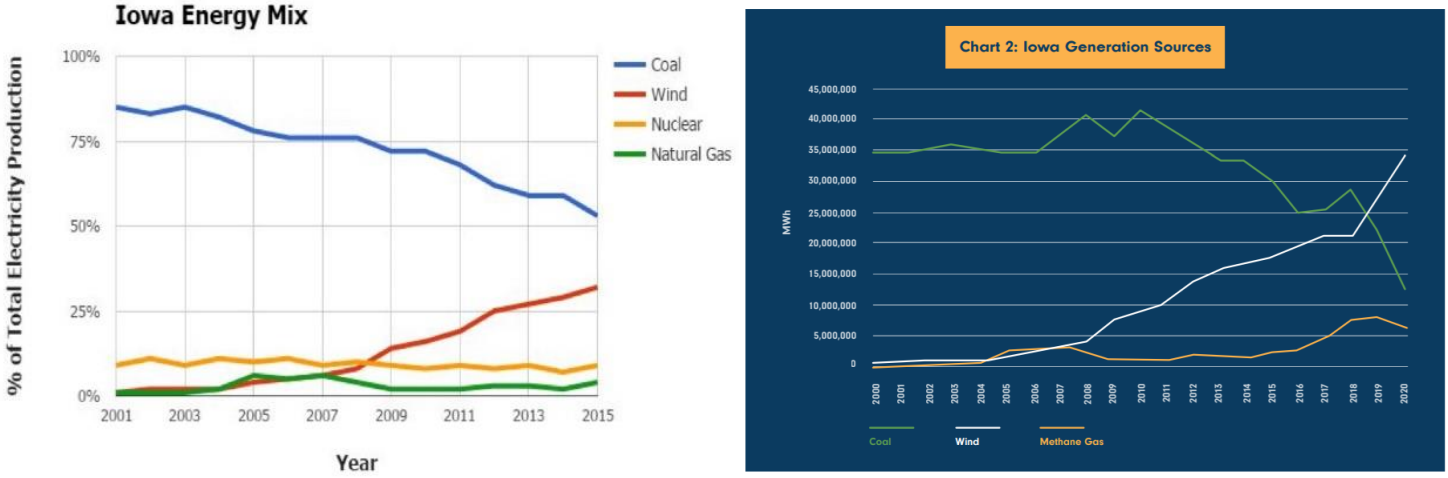

Fig. 12b: Changes in Iowa Energy Mix

Vermont is so low because it had only one small fossil-fired unit (a diesel unit), and it was a peaker and so did not often run [34]. Almost 75% of Vermont's electric energy came from a large nuclear facility (Vermont Yankee) and most of the rest came from outside the state via the ISO-NE market. This nuclear plant was retired in 2014, and this slightly increased their emissions in 2015, but their emissions are almost zero in 2022.

6.0 Heat rates

The values of Table 2 (fuel cost table) reflect only the cost of fuel input to a generation plant; they do not reflect the actual costs of producing electrical energy as output from the plant because substantial losses occur during production. Some power plants have overall efficiencies as low as 30%; in addition, the plant efficiency varies as a function of the generation level P_g. We illustrate this point in what follows.

We represent plant efficiency by η. Then η=energy output/energy input. We obtain η as a function of P_g by measuring the energy output of the plant in MWhrs and the energy input to the plant in MBTU.

We could get the energy output by using a wattmeter to obtain P_g over a given period of time, say an hour, and we could get the energy input by measuring the coal tonnage used during the hour and then multiplying by the coal energy content in MBTU/ton.

We could then plot the fuel input in MBTU/hr as a function of the power output P_g in MW. Such a plot is called an *input-output curve*, indicating how much fuel rate is required to produce a power level. A typical input-output curve is shown in Fig. 13. We denote fuel rate (input, vertical axis of Fig. 13) as R (W&W [35] denote fuel rate as H – see p. 8 in W&W).

One notes that the I/O curve of Fig. 13 does not go to P_g=0. A generating unit has a minimum stable output, typically 10-30% for oil and natural gas-fired steam units and 20-40% for coal-fired steam units [36].

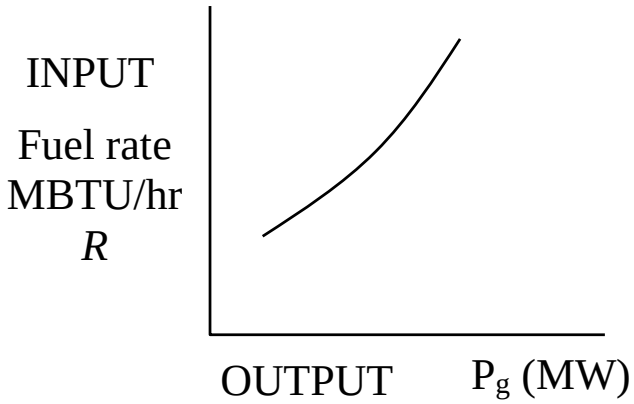

Fig. 13: Input-output curve

One interesting feature with respect to Fig. 13 is that as fuel input is increased, the power output per unit fuel input begins to decrease. We can see this more clearly if we invert the axes, as in Fig. 14, yielding a *production function*, where, for high enough fuel rates, we will get no additional power output.

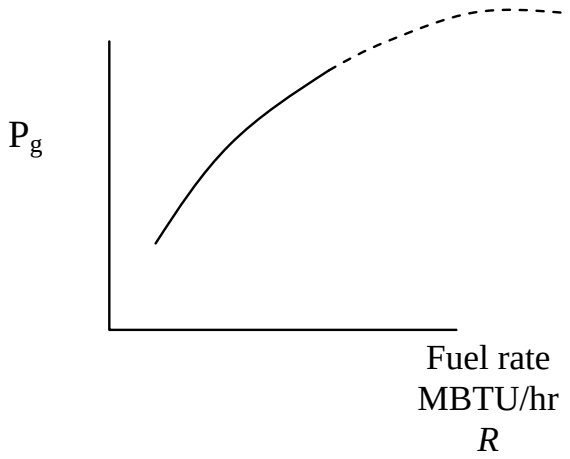

Fig. 14: Production function

Physically, this happens because the furnace, boiler, steam pipes leak a larger percentage of input heat as temperatures increase. Economists call this the [37]

law of diminishing marginal product: for most processes (fertilizer/crops workers/factories), the rate of increase in output decreases as the input increases, assuming other inputs are fixed.

To obtain η, we want the output energy divided by the input energy, which is

$$\eta \sim P_g \div R$$

which in terms of units is MW ÷ MBTU/hr to give units of MWhr/MBTU. Notice that these units are energy/energy, as they should be when computing η. However, the MBTU and MWhr are different units of energy, and so we are not getting η exactly, but we are getting something proportional to η.

So let's obtain the ratio of the power to the fuel rate ($P_g \div R$) for every point on the input-output curve, and plot the results against P_g. Fig. 15 shows a plot of the ratio P_g/R (units of MWHR/MBTU) versus P_g.

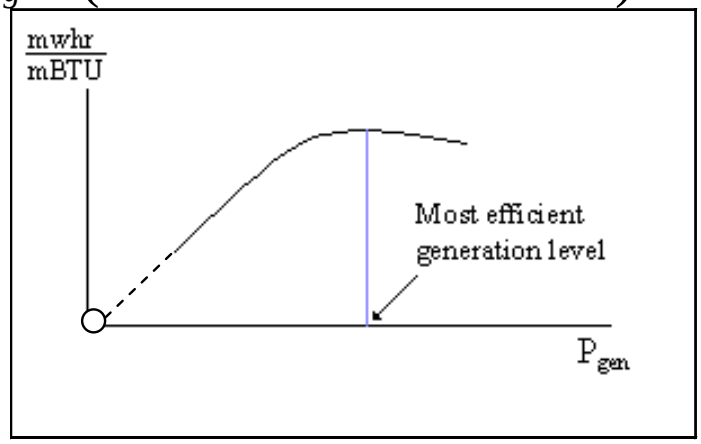

Fig. 15: Plot of MWhr/MBTU vs. P_g

Fig. 15 indicates that efficiency is poor for low generation levels (a connected plant that is operating at zero MW output still has to supply station loads) and increases with generation, but at some optimum level it begins to diminish. Most power plants are designed so that the optimum level is close to the rated output.

The *heat rate* curve is similar to Fig. 15 except that the y-axis is inverted to yield MBTU/MWhrs, which is proportional to $1/\eta$. This curve is illustrated in Fig. 16. We denote heat rate by H. (W&W [35] use H for fuel rate). Since the heat rate depends on operating point, we write $H=H(P_g)$.

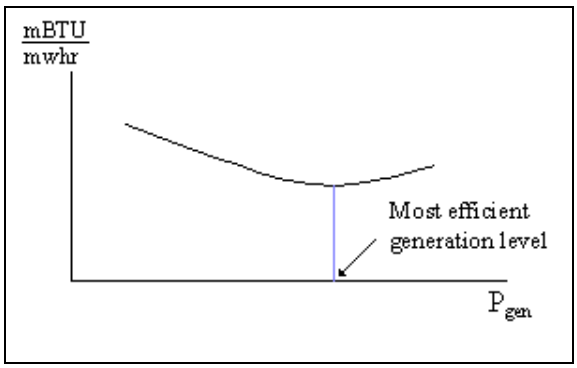

Fig. 16: Plot of Heat Rate (H) vs. Generation (P_g)

Some typical heat rates for units at maximum output are (in MBTU/MWhrs) 9.5-10.5 for fossil-steam units and nuclear units, 13.0-15.0 for combustion turbines [38], and 7.0-9.5 for combined cycle units. Future combined cycle units may reach heat rates of 6.5-7.0. *It is important to understand that the **lower** the heat rate, the more efficient the unit*.

An easy way to remember the meaning of heat rate $H=H(P_g)$ is it is the amount of input energy (MBTU) required to produce a MWhr, at generation level P_g.

How does H relate to efficiency? To answer this question, we need to know that there are 1054.85 joules per BTU.

$$\frac{1}{\eta} \sim H\,\frac{MBTU}{MWhr} = H\,\frac{1E6}{1E6}\,\frac{BTU}{Whr} = H\,\frac{BTU\,(1054.85\,j/BTU)}{(j/\sec)3600\sec}$$

$$\Rightarrow \frac{1}{\eta} = H\,\frac{1054.85}{3600} = \frac{H}{3.41} \Rightarrow H = \frac{3.41}{\eta}$$

Observe: We have seen this before when we computed CO_2 emissions per MWhr out (see pg. 26), e.g., for the NGCC plant:

$$117.08\,\frac{lbs}{MBTU_{IN}} \times \frac{1MBTU_{IN}}{.58MBTU_{OUT}} \times \frac{3.41MBTU}{MWhr} = 688.5lbs/MWhr$$

We can see now that the above calculation can be thought of as

$$117.08\,\frac{lbs}{MBTU_{IN}} \times \frac{3.41MBTU_{IN}}{.58MBTU_{OUT}} = \frac{3.41MBTU_{IN}}{\eta MBTU_{OUT}} = 688.5lbs/MWhr$$

or

$$117.08\,\frac{lbs}{MBTU_{IN}} \times H = 688.5lbs/MWhr$$

where H in this case is 3.41/.58=5.88 MBTU/MWhr.

The heat rate curve is a fixed characteristic of the plant, although it can change if the cooling water temperature changes significantly (engineers may sometimes employ

seasonal heat rate curves). The heat rate curve may also be influenced by the time between maintenance periods as steam leakages and other heat losses accumulate.

The above use of the term "heat rate" is sometimes also called the "**average heat rate**." This is because we get it by dividing absolute values of fuel input rate by absolute values of electric output power. For example, if you buy an apple at $50 and a second one at $10, the average cost of apples after buying the first apple is $50/apple but after buying the second apple is $(50+10)/2=$30/apple.
This is different than **incremental heat rate**, as will be illustrated in the following example.

Example [39]: Consider the input-output curve for Plant X in Fig. 17.

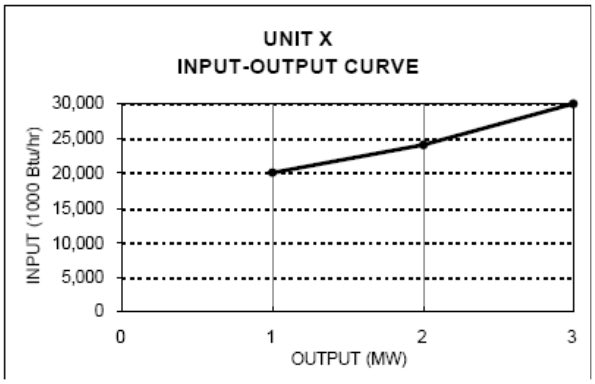

Fig. 17

Compute the average heat rate characteristic and the incremental heat rate characteristic.

Average heat rates are computed by dividing the fuel rate by the generation level, $H=R/P_g$, as follows:

Block 1: 20,000/1=20,000
Block 2: 24,000/2=12,000
Block 3: 30,000/3=10,000

Incremental heat rates computed by dividing the increment of fuel rate by the increment of power, $IH=\Delta R/\Delta P_g$ as follows:

Block 1: 20,000/1=20,000
Block 2: 4,000/1=4,000
Block 3: 6,000/1=6,000

These results are summarized in Table 9 below:

Table 9

	CAPACITY (MW)	INPUT-OUTPUT CURVE (1000 Btu/hr)	INCREMENTAL HEAT RATE (Btu/kWh)	AVERAGE HEAT RATE (Btu/kWh)
BLOCK 1	1	20,000	20,000	20,000
BLOCK 2	2	24,000	4,000	12,000
BLOCK 3	3	30,000	6,000	10,000

Fig. 18 below illustrates the input-output curve, the average heat rate curve, and the incremental heat rate curve.

FIGURE 2A: HEAT RATE PLOTS FOR UNIT X

	Output (MW)	Input-Output Curve (1000 Btu/hr)	Incremental Heat Rate (Btu/kWh)	Average Heat Rate (Btu/kWh)
BLOCK 1	1	20,000	20,000	20,000
BLOCK 2	2	24,000	4,000	12,000
BLOCK 3	3	30,000	6,000	10,000

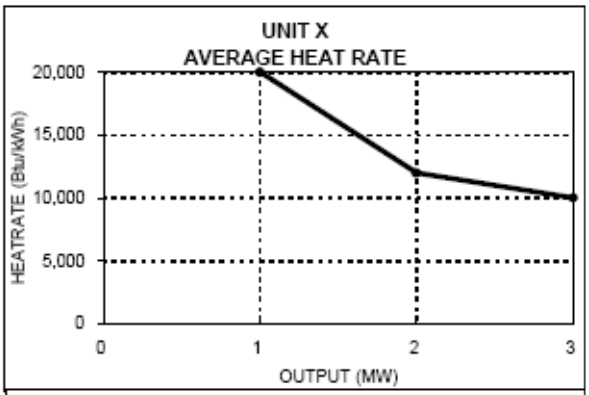

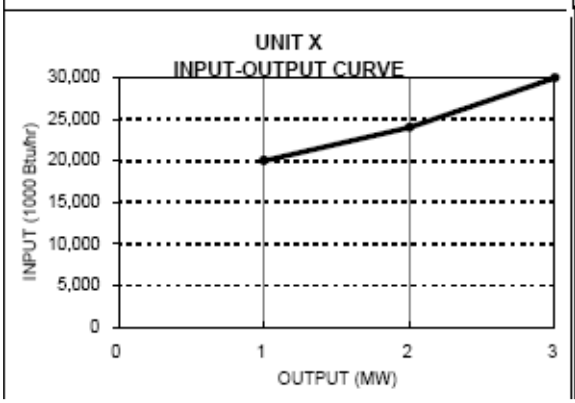

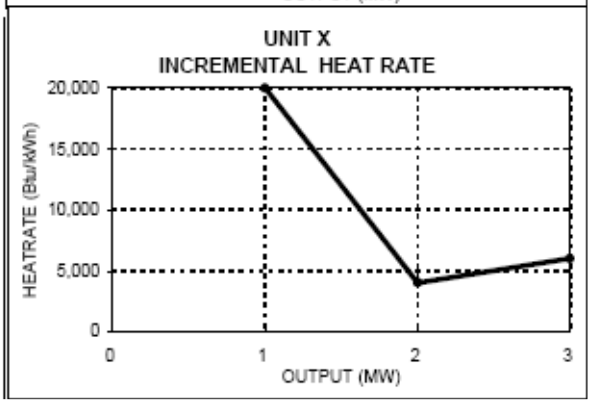

Fig. 18

We should note, however, that our first incremental heat rate value of 20,000 has a problem. This value assumes that the I/O curve extends as shown on the left hand side in Fig. 19 below. Probably a better approximation would be to extend it as indicated on the right hand side of Fig. 19.

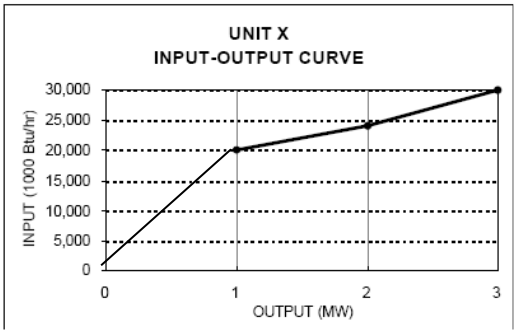

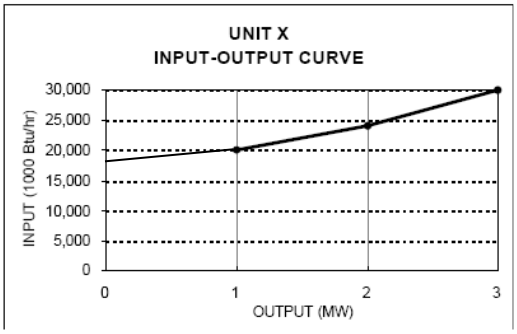

Fig. 19

Actually, it does not extend to 0 MW output because the unit, like all real units, has a min generation level.

Although you may see data entered which reflects a "high initial incremental value," you should know that a value so computed does not represent a true incremental heat rate value at all.

Reference [39] provides data for units in California. The one below, Fig. 20, was at one time one of the most efficient gas-fired units in the PG&E system. On the coast about 100 miles south of San Francisco, a supercritical plant, it is called Moss Landing Unit 7.

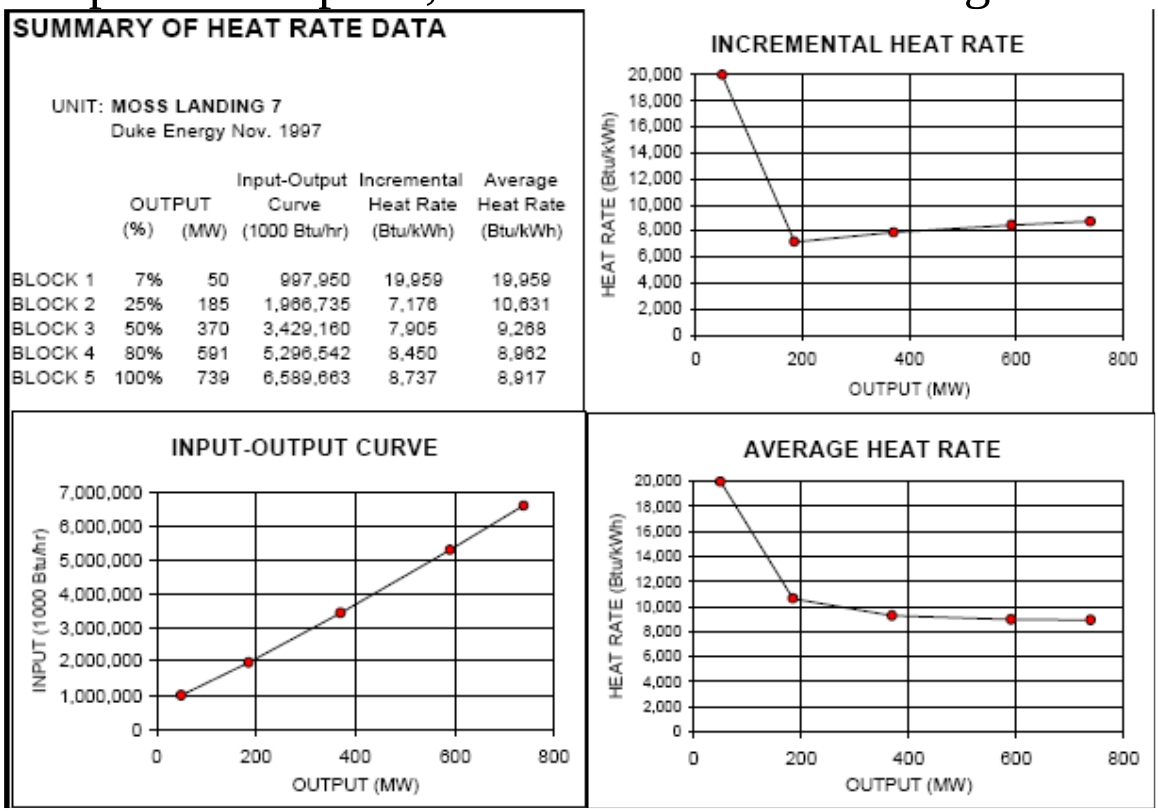

SUMMARY OF HEAT RATE DATA

UNIT: **MOSS LANDING 7**
Duke Energy Nov. 1997

	OUTPUT (%)	OUTPUT (MW)	Input-Output Curve (1000 Btu/hr)	Incremental Heat Rate (Btu/kWh)	Average Heat Rate (Btu/kWh)
BLOCK 1	7%	50	997,950	19,959	19,959
BLOCK 2	25%	185	1,966,735	7,176	10,631
BLOCK 3	50%	370	3,429,160	7,905	9,268
BLOCK 4	80%	591	5,296,542	8,450	8,962
BLOCK 5	100%	739	6,589,663	8,737	8,917

Fig. 20

Note that the Moss Landing unit 7 full-load average heat rate is 8.917 MBTU/MWhr, which gives an efficiency of 3.41/8.917=38.2%. This is pretty good.

The next one, Fig. 21, is an old oil-fired unit in San Francisco called Hunter's Point.

SUMMARY HEAT RATE DATA

UNIT: HUNTERS POINT 3

	OUTPUT (%)	OUTPUT (MW)	Input-Output Curve (1000 Btu/hr)	Incremental Heat Rate (Btu/kWh)	Average Heat Rate (Btu/kWh)
BLOCK 1	9%	10	210,370	21,037	21,037
BLOCK 2	25%	27	378,378	9,883	14,014
BLOCK 3	50%	54	671,436	10,854	12,434
BLOCK 4	80%	86	1,083,476	12,251	12,366
BLOCK 5	100%	107	1,347,986	13,548	12,598

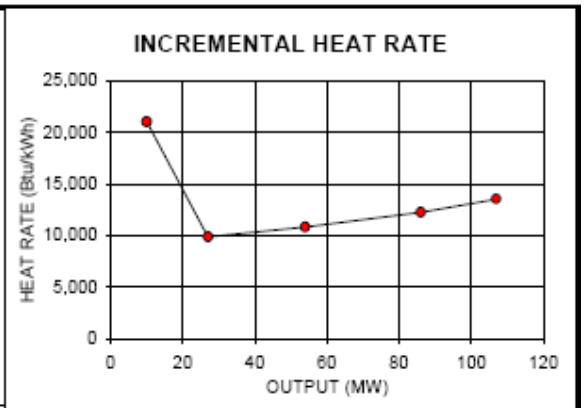

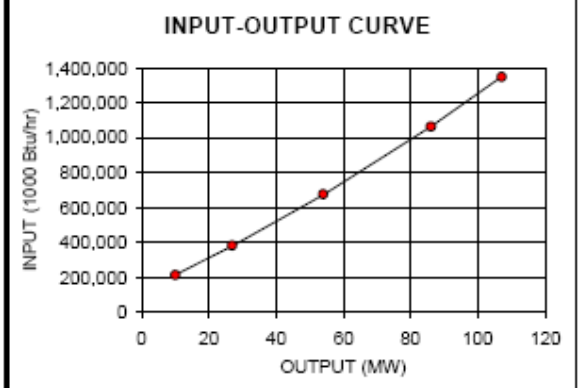

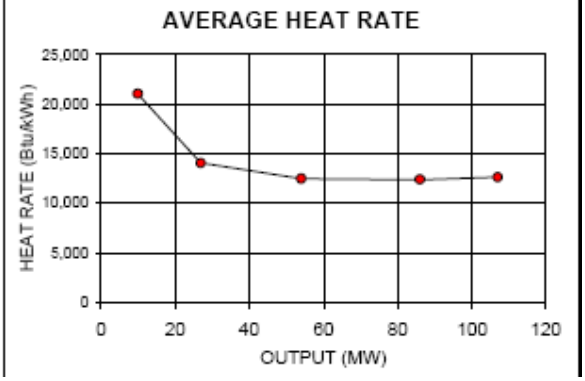

Fig. 21

Note the full-load average heat rate of this plant is 12.598 MBTU/MWhr, which corresponds to an efficiency of 3.41/12.598=27.1%.

Hunter's point was built in 1927 and demolished in 2008. Moss Landing Unit 7 was built in 1964 and retired in 2016, following installation of two combined cycle plants (Units 1 and 2) in 2002.

7.0 Cost rates

We are primarily interested in how the cost per MWhr changes with P_g, because that will tell us something about how to achieve the most economic dispatch of generation for a given demand (we will see that optimality is achieved when marginal or incremental costs of all regulating units are equal).

To get cost per MWhr as a function of P_g, we assume we know K, the cost of the input fuel in $/MBTU. Also, recall that

- R is the rate at which the plant uses fuel, in MBTU/hr (which is dependent on P_g) – it is just the input-output curve (see Fig. 13).

And we will denote

- C as the cost per hour in $/hour.

Then, if $H(P_g)$, the heat rate, is the input energy used per MW per hour, then multiplying H by P_g gives input energy per hour, i.e., $R=P_gH(P_g)$ where H must be evaluated at P_g. So $C(P_g)=R(P_g)K=P_gH(P_g)K$, i.e., the cost rate function $C(P_g)$ is just the fuel rate function $R(P_g)$ scaled by the fuel cost K.

A typical plot of $C(P_g)$ vs. P_g is illustrated in Fig. 22. For single cycle power plants, $C(P_g)$ is represented as a quadratic and therefore convex, i.e., the set of points lying on or above $C(P_g)$ contain all line segments between any pair of points.

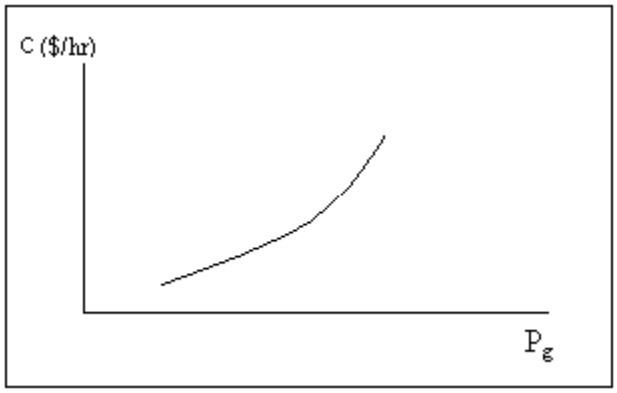

Fig. 22: Plot of cost per hr (C) vs. generation (P_g)

Fig. 22 shows that cost/hour increases with generation, a feature one expects since higher generation levels require greater fuel intake per hour.

The **incremental cost curve for the plant** can be obtained by differentiating the plot in Fig. 22, i.e., by computing dC/dP_g. A typical incremental cost curve is shown in Fig. 23. Note that because C is convex, dC/dP_g is a non-decreasing function.

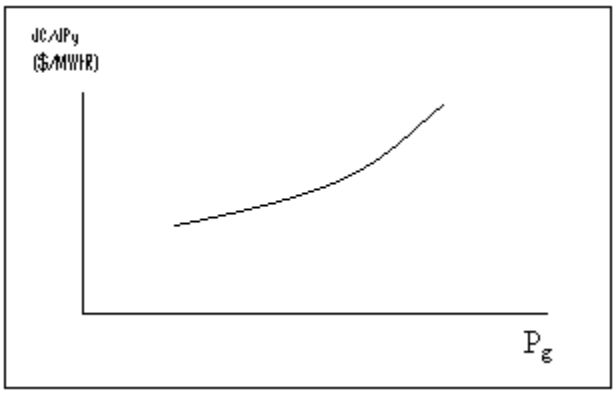

Fig. 23: Plot of incremental cost dC/dP_g vs. gen P_g

One last thing about getting incremental cost. Recall that the cost per hour is given by $C(P_g) = R(P_g)K$, where $R(P_g)$ is just the input-output curve. Therefore $IC=dC/dP_g=K(dR/dP_g)$. The derivative dR/dP_g is the incremental heat rate, which we denoted by $IH(P_g)$. Therefore, in summary:

$$C(P_g)=R(P_g)K=P_gH(P_g)K$$
$$IC=dC(P_g)/dP_g=(dR(P_g)/dP_g)K=IH(P_g)K$$

Example 1

An 100 MW coal-fired plant uses a type of coal having an energy content of 12,000 BTU/lb. The coal cost is $1.5/MBTU. Typical coal usage corresponding to the daily loading schedule for the plant is as follows:

Table 10

Time of Day	Electric Output (MW)	Coal Used (tons)
12:00am-6:00am	40	105.0
6:00am-10:00am	70	94.5
10:00am-4:00pm	80	156.0
4:00pm-12:00am	100	270.0

For each of the four load levels, find (a) the efficiency η, (b) the avg heat rate H (MMBTU/MWhr), (c) the cost per hour, C ($/hr). Also, for the loading levels of 40, 70, and 80 MW, use a piecewise linear plot of C vs P to obtain incremental cost IC as a function of unit loading P. Then plot incremental cost as a function of unit loading. The conversion factor from joules to BTU is 1054.85 joules/BTU, and the units for coal used, tons, are short-tons, 2000 lb/ton.

Solution

Let T be the number of hours the plant is producing P MW while using y tons of coal. We need to compute the total energy out of the plant and divide by the total energy into the plant, but we need both numerator and denominator to be in the same units. We will convert both to joules (recall a watt is a joule/sec).

(a) $$\eta = \frac{P \text{ MW} \times T \text{ hr} \times \left(10^6 \frac{\text{watts}}{\text{MW}} \times 3600 \frac{\text{sec}}{\text{hr}} \right)}{y \text{ tons} \times \left(2000 \frac{\text{lb}}{\text{ton}} \times 12{,}000 \frac{\text{BTU}}{\text{lb}} \times 1054.85 \frac{\text{joules}}{\text{BTU}} \right)}$$

Note that the above expression for efficiency is dimensionless.

(b) The average heat rate is the amount of MBTUs used in the amount of time T divided by the number of MW-hrs output in the amount of time T.

$$H = \frac{y \text{ tons} \times \left(2000 \frac{\text{lb}}{\text{ton}} \times 12,000 \frac{\text{BTU}}{\text{lb}} \times \frac{1\text{MBTU}}{10^6 \text{BTU}} \right)}{P \times T}$$

We can use the expressions for H and η to show that $H = \frac{1}{\eta} \times \frac{3600}{1054.85} = \frac{3.41}{\eta}$, in units of MBTU/MWhr (also see p. 34). Thus, if a unit is 100% efficient, then it will have a heat rate of 3.41 MBTU/MWhr, the absolute best (lowest) heat rate possible.

(c) $C = RK$ where R is the rate at which the plant uses fuel and K is fuel cost in \$/MBTU. Note from units of P and H that
$R = PH$ ➔ $C = PHK$ where H is a function of P.

Application of these expressions for each load level yields the following results:

Table 11

T (hrs)	P (MW)	y (tons)	η	H (mbtu/mwhr)	C ($/hr)
6	40	105.0	0.33	10.5	630
4	70	94.5	0.42	8.1	850
6	80	156.0	0.44	7.8	936
8	100	270.0	0.42	8.1	1215

To obtain incremental cost $IC = \frac{dC}{dP}$, we can plot C vs. P and then get an approximation on the derivative by assuming a piecewise linear model as shown in Figure 24.

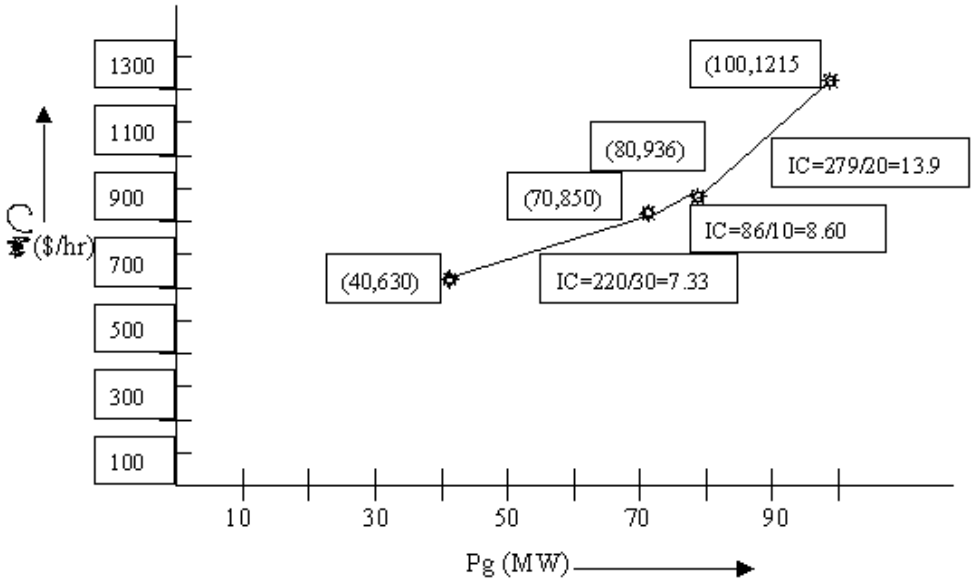

Figure 24: Calculation of Incremental Cost

The incremental costs are plotted as a function of loading in Fig. 25.

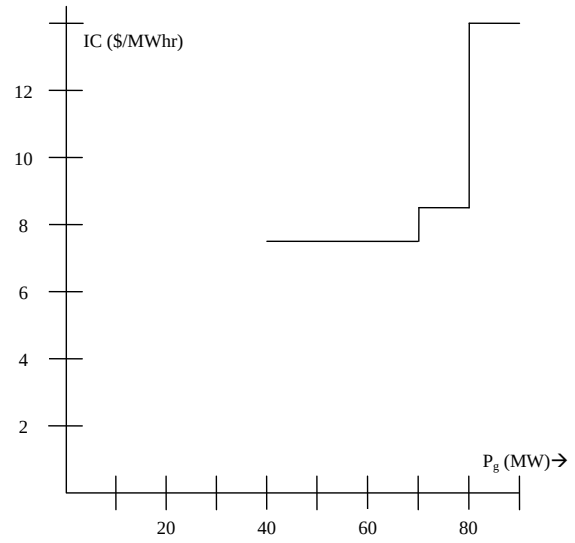

Fig 25: Incremental cost curve from piecewise-linear cost curve

We may use another procedure to model the incremental costs. In this procedure, we first fit the data to a quadratic polynomial. Matlab commands for doing so are below:

```
>> p=[40      70   80   100]';
>> c=[630     850 936 1215]';
>> X = [ones(size(p))  p  p.^2];
>> a=X\c
a =
  604.8533
   -2.9553
    0.0903
>> T = (0:1:100)';
>> Y = [ones(size(T))  T  T.^2]*a;
```

>> plot(T,Y,'-',t,y,'o'), grid on

The quadratic function is therefore

$$C(P)=0.0903P^2-2.9553P+604.85$$

Figure 26 shows the plot obtained from Matlab.

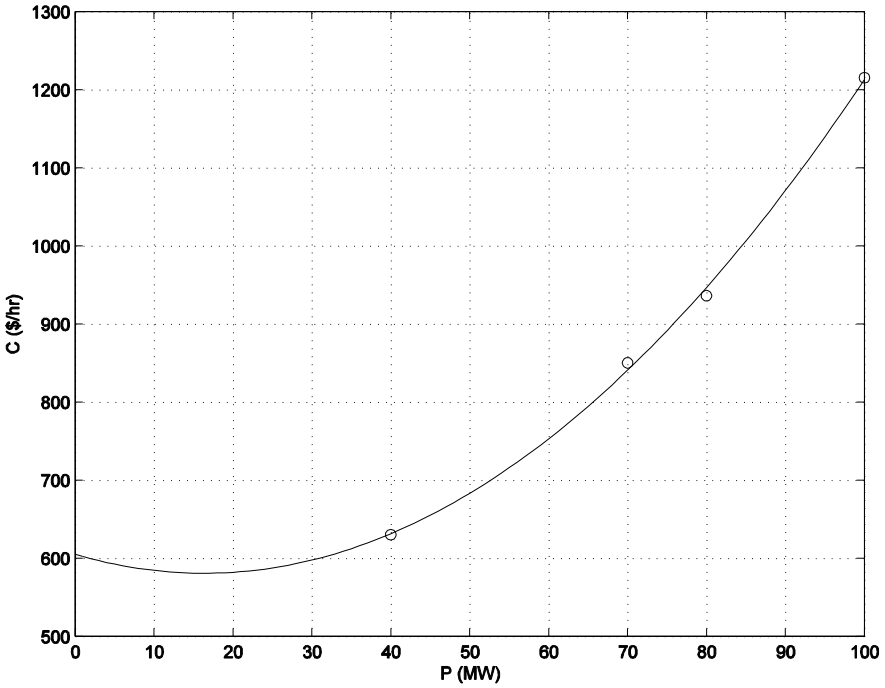

Fig 26: Quadratic Curve Fit for Cost Rate Curve

Clearly, the curve is inaccurate for very low values of power (note it is above \$605/hr at P=0 and decreases to about \$590/hr at P=10). We can get the incremental cost curve by differentiating $C(P)$:

$$IC(P)=0.1806P-2.9553$$

This curve is overlaid on the incremental cost curve of Fig. 25, resulting in Fig. 27. Both linear and discrete functions are approximate. Although the linear one appears more accurate in this case, it would be easy to improve accuracy of the discrete one by taking points at smaller intervals of P_g. Both

functions should be recognized as legitimate ways to represent incremental costs. The linear function is often used in traditional economic dispatching; the discrete one is typical of market-based offers.

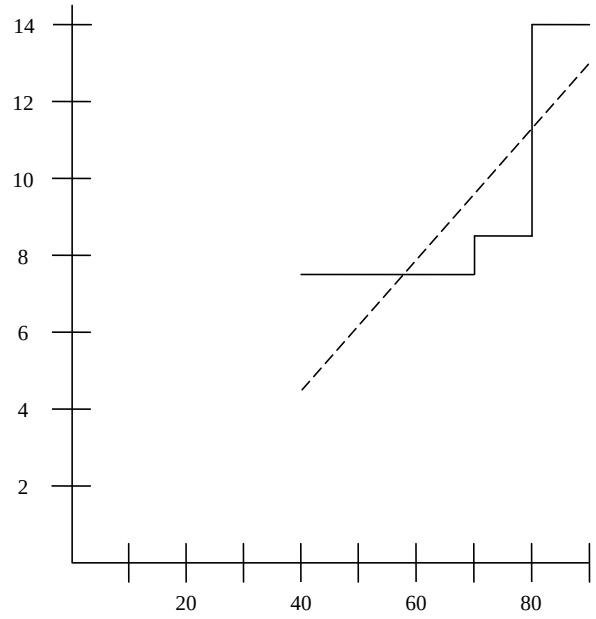

Fig. 27: Comparison of incremental cost curve obtained from piecewise linear cost curve (solid line) and from quadratic cost curve (dotted line)

8.0 Market-based offers

As indicated in the last section, electricity markets typically allow only piecewise linear representation of generator incremental cost curves.

The real-time and the day-ahead markets are implemented via computer programs based on optimization theory. The program used for the real-time market is called the security-constrained economic dispatch (SCED). This program, the SCED, is used together with a program called

the security-constrained unit commitment (SCUC) program for the day-ahead market. Both SCED and SCUC also solve for ancillary service prices through a formulation known as co-optimization. The seven US market operators publish real-time displays of their locational marginal prices (LMPs). Fig. 28a shows a snapshot of prices for Monday, 2/15/2021 (computed from SCED and found at www.misoenergy.org/markets-and-operations/real-time--market-data/markets-displays/), where we observe, due to the extremely cold temperatures, most prices are very high throughout the region, although the prices in southern Indiana, Arkansas, & Louisiana are much lower. The real time MISO display (see above URL) indicates LMP as well as marginal loss component (MLC) and marginal congestion component (MCC), where

$$\mathbf{LMP = MEC + MCC + MLC} \qquad \mathbf{(*)}$$

The MEC is the marginal energy component. Inspection of the MCC and MLC given at the MISO real-time displays indicates that high LMPs are caused by high MECs, but the extremely low LMPs are caused by large and negative MCCs. What we can conclude from this observation is that

- The system is using expensive units to supply energy;
- In the blue/yellow areas, a negative MCC (congestion) price is offsetting the high energy prices. The negative MCC means that load should be increased (i.e., generation should be decreased) within that area.

This situation is related to the cold weather effect on G&T outages, see [40] and the 2/15/21 article [41], which states:

> The Midcontinent Independent System Operator (MISO) also confirmed it directed Entergy to shed load in Texas on Feb. 15. "Sustained frigid temperatures and winter weather impacting the [MISO] South Region contributed to the loss of generation and transmission. This led to emergency actions in the region's western portion to avoid a larger power outage on the bulk electric system," it said.

There are both very high and very low prices in the same overall condition illustrated in Fig. 28a. The high prices occur because the demand is extremely high and so the highest-priced units are setting the price (LMPs are set by the last offer accepted; this will be the highest priced offer accepted). The low prices occur because generation in those areas has been increased to the point that nearby transmission is congested, causing negative MCCs that cause congestion prices that incentivize the generation in the area to decrease.

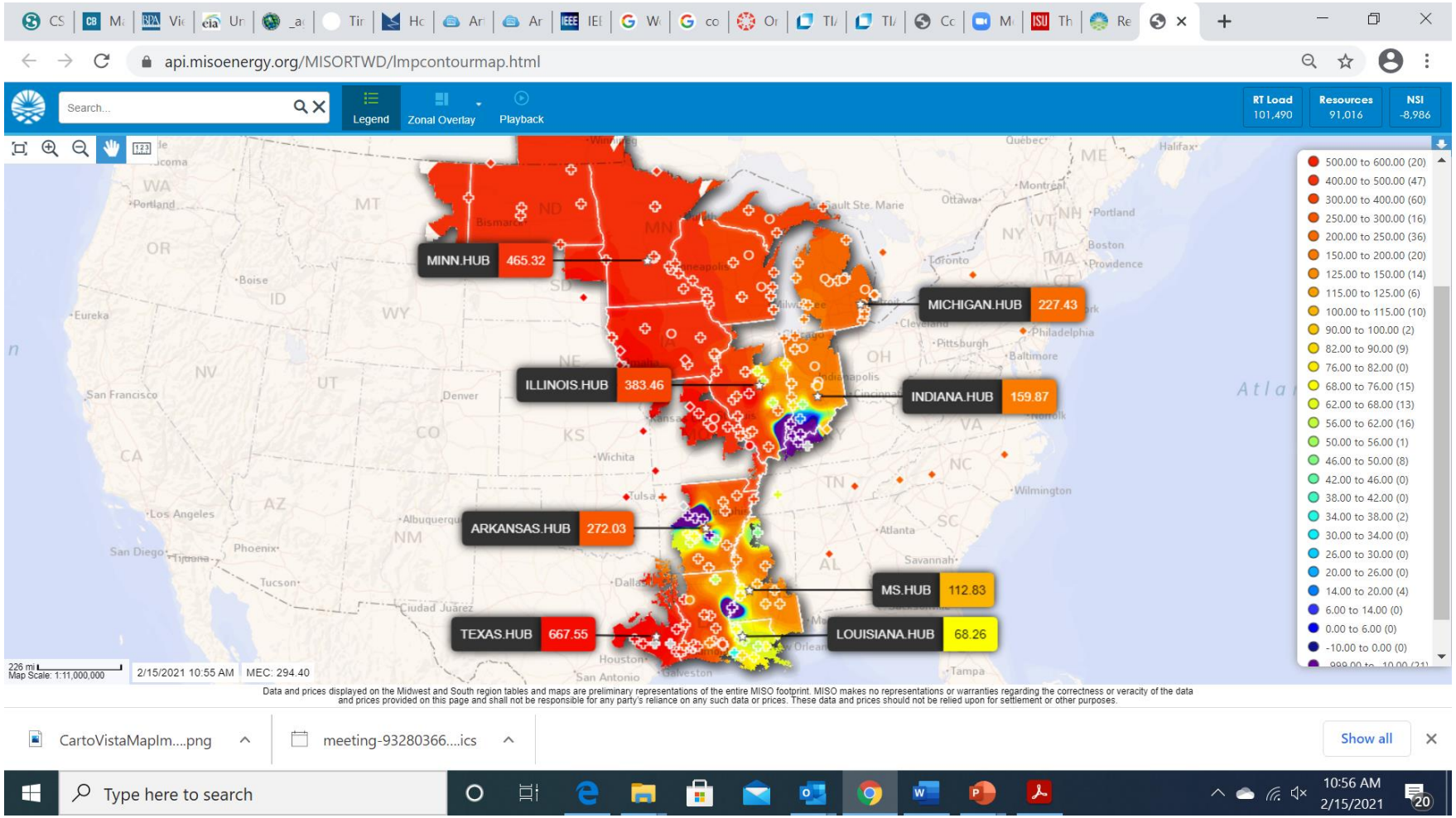

Fig. 28a: MISO LMPS for 2/15/2021, 10:55amCT

Fig. 28b below shows a much less extreme condition, relative to Fig. 28a. This is because it represents a moderate meteorological condition (about 37° F, 10 mph winds), and so lower cost (relative to the condition of Fig. 28a) generation is setting the price. There is congestion here as well, e.g., in northwest Iowa, but it is because of the abundance of low-cost wind that is there.

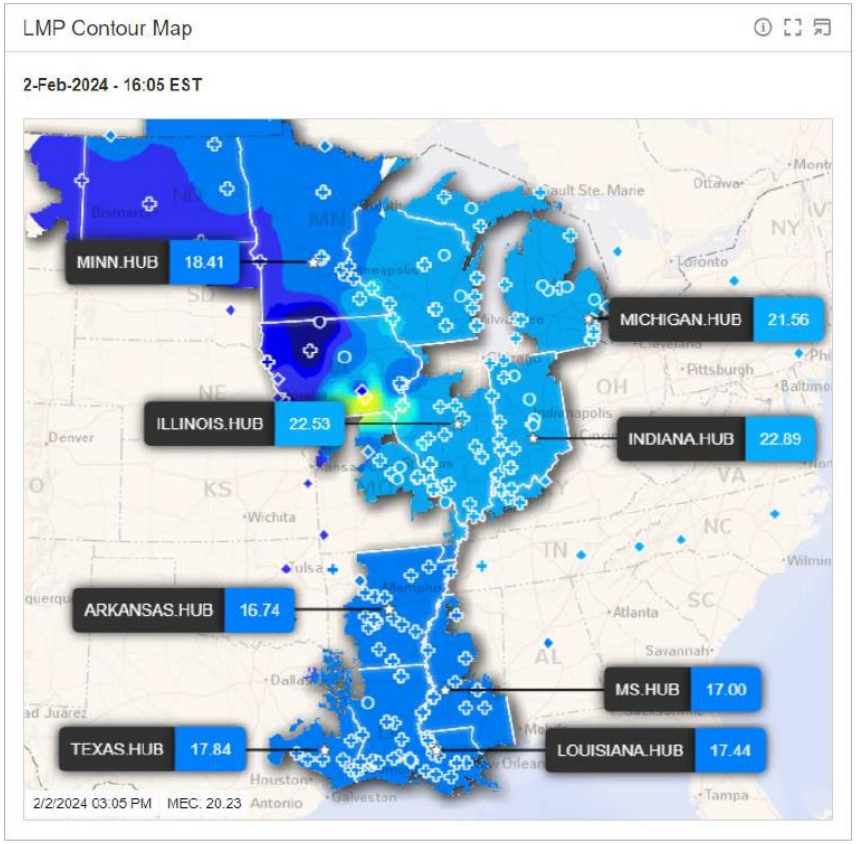

ExAnte LMP

02-Feb-2024 - Interval 16:10 EST

Name	LMP	MCC	MLC
ARKANSAS.HUB	15.91	-8.86	-1.10
ILLINOIS.HUB	28.40	2.65	-0.12
INDIANA.HUB	29.02	1.77	1.38
LOUISIANA.HUB	16.73	-8.93	-0.21
MICHIGAN.HUB	27.60	0.00	1.73
MINN.HUB	21.88	-2.72	-1.27
MS.HUB	16.21	-8.87	-0.79
SWPP	14.64	-8.66	-2.57
TEXAS.HUB	17.25	-9.03	0.41

Fig. 28b: MISO LMPS for 2/2/2024, 3:05pmCT

We will say no more about SCED and SCUC at this point; this topic is further addressed in EE 458 and EE 553. Instead, we will provide a simple, conceptual description of how energy market prices are determined. This description is based on standard microeconomic theory but can be followed without background in microeconomics. However, the description necessarily omits some important concepts related to losses and congestion. The discussion focuses only on the MEC component.

The following example is adapted from [42]. Consider that our electric energy market has three buyers, B1, B2, B3 and two sellers, S1, S2. The buyers represent load-serving entities, and the sellers represent generation owners. Consider that these buyers and sellers submit their bids (to buy) and their offers (to sell) via an internet system as shown in Fig. 28c.

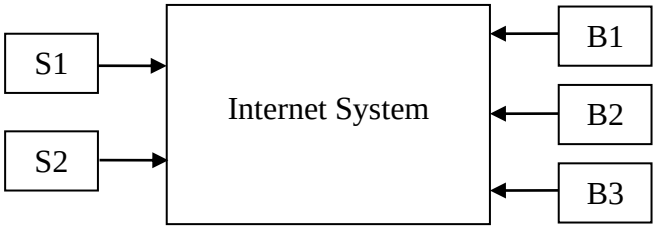

Figure 28c: Illustration of buyer-seller interaction with internet-based market

Each seller has energy to sell, but the price at which they are willing to sell increases with the amount they sell. This is a reflection of the fact that the cost of producing 1 more unit of energy (MWhr) increases as a unit is loaded higher.

Likewise, each buyer wants to purchase energy, but the price each buyer is willing to pay to obtain the energy decreases with the amount that they buy. This reflects that our first unit of energy is used to supply our most critical needs, and after those needs are satisfied, the next units of energy are used to satisfy less critical needs, so we are unwilling to pay as much for them.

Table 12 illustrates a representative set of bids and offers submitted by buyers and sellers.

Table 12: Offers and bids for examples

Offers to sell		Bids to buy		
S1	S2	B1	B2	B3
$10.00	$10.00	$70.00	$70.00	$25.00
$50.00	$50.00	$70.00	$50.00	0
$65.00	$70.00	$65.00	$25.00	0
$70.00	$70.00	$65.00	0	0
∞	∞	0	0	0
∞	∞	0	0	0
∞	∞	0	0	0

Once each buyer/seller enters their data according to Table 12, the internet system reconstructs it according to Table 13.

Table 13: Reconstructed offers and bids

Offer/bid order	Offers to sell 1 MWhr		Bids to buy 1 MWhr	
	Seller	Price	Buyer	Price
1	S1	$10.00	B1	$70.00
2	S2	$10.00	B1	$70.00
3	S1	$50.00	B2	$70.00
4	S2	$50.00	B1	$65.00
5	S1	$65.00	B1	$65.00
6	S2	$70.00	B2	$50.00
7	S1	$70.00	B2	$25.00
8	S2	$70.00	B3	$25.00

We can visualize the data in Table 13 by plotting the price against quantity for the offers and for the bids. This provides us with the supply and demand schedules of Figure 29 [42].

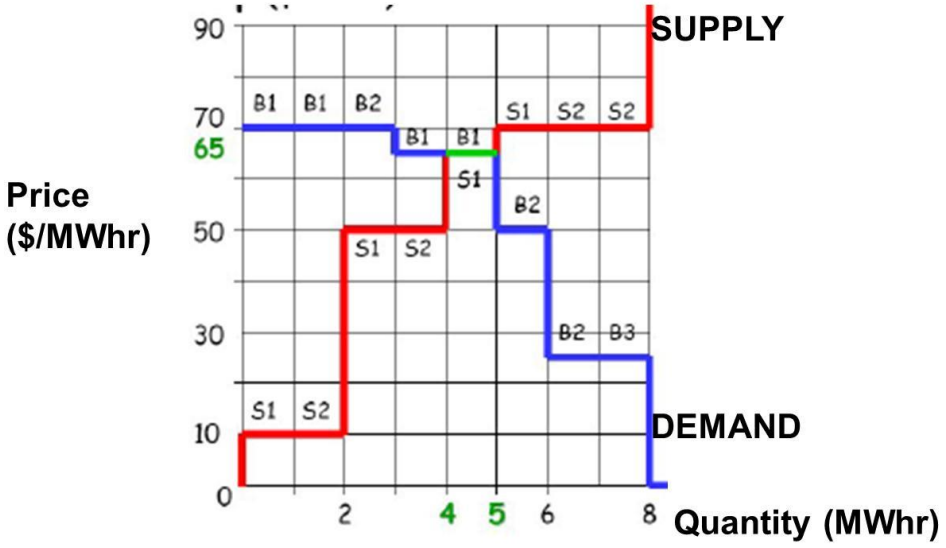

Figure 29: Supply-demand schedules illustrating electricity market operation [42]

The point (or those points) where the supply schedule intersects the demand schedule determines the market clearing price. This is the price that all sellers are paid to supply their energy, and it is the price that all buyers pay to receive their energy. In Figure 29, this price is $65/MWhr. It is the very best price to choose because it maximizes the total “satisfaction” felt by the buyers and sellers.

This satisfaction, for the sellers, can be measured by the difference between the price they offered and the price they were actually paid for the energy they supplied. If we add up all of these differences for all sellers, then we obtain the net seller surplus. This satisfaction, for the buyers, can be measured by the difference between the price they bid and

the price they actually had to pay for the energy they received. If we add up all of these differences for all sellers, then we obtain the net buyer surplus. The net seller surplus and the net buyer surplus are illustrated in Fig. 30 [42].

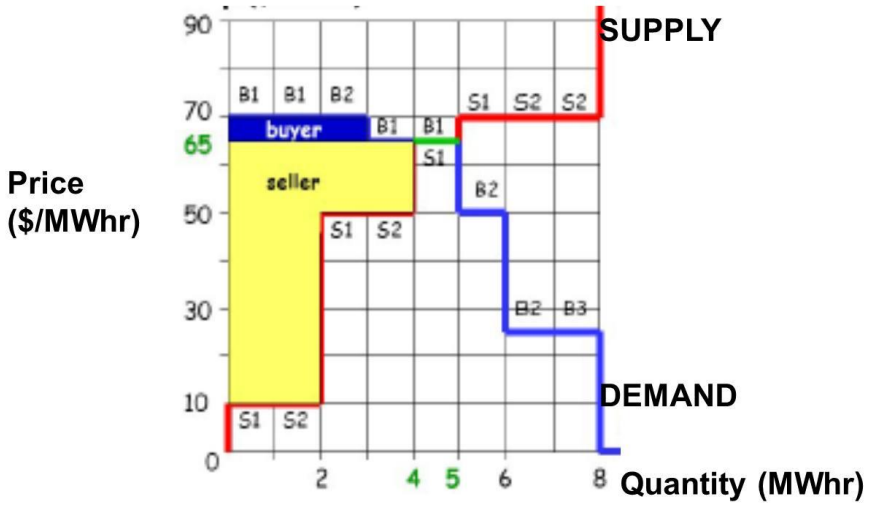

Figure 30: Illustration of net seller & net buyer surplus [42]

The total net surplus is the sum of the buyer and seller net surpluses. The market clearing price is the price that maximizes the total net surplus.

In Fig. 30, the quantity traded could be either 4 or 5 MWhrs, but the 5th MWhr would neither increase nor decrease total net surplus. The decision on whether to trade 4 or 5 MWhrs in such a case is determined by market rules.

The example of this section illustrates the way electricity markets would clear if there are no losses and if the transmission capacity of each line was infinite. One conceptualization of such a situation is when all generators and all loads are located at the same electric node. In such a case, there is a single price by which all sellers are paid and all buyers pay.

We repeat equation (*) here:

$$\mathbf{LMP = MEC + MCC + MLC} \qquad \mathbf{(*)}$$

observing that with MCC=MLC=0, as it is in the above example, then LMP=MEC. That is, the price of $65/MWhr is the MEC, and since there is no congestion and no losses, it is also the LMP.

In reality, of course, each transmission circuit does have some resistance and therefore incurs some losses as current flows through it, and each transmission circuit also has an upper bound for the amount of power that can flow across it. These two attributes, losses and transmission limits, result in locational variation in prices throughout the network, which are called, as we have already seen, the locational marginal prices (LMPs).

9.0 Effect of Valve Points in Fossil-Fired Units

Figures 22 and 24 well represent cost curves of small steam power plants, but actual cost curves of large steam power plants differ in one important way from the curves shown in Figs. 22 and 24 – they are not smooth! The light curve of Fig. 31 [43] more closely captures the cost variation of a large steam power plant.

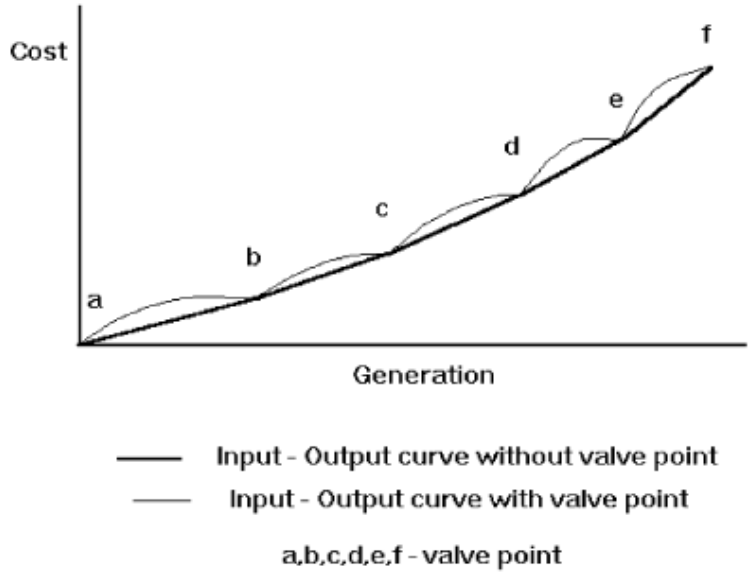

Fig. 31: Cost rate curve for large steam power plant [43]

The reason for the discontinuities in the cost curve of Fig. 31 is because of multiple steam valves. In this case, there are 5 different steam valves. Large steam power plants are operated so that valves are opened sequentially, i.e., power production is increased by increasing the opening of only a single valve, and the next valve is not opened until the previous one is fully opened. So the discontinuities of Fig. 31 represent where each valve is opened.

The cost curve increases at a greater rate with power production just as a valve is opened. The reason for this is that the so-called throttling losses due to gaseous friction around the valve edges are greatest just as the valve is opened and taper off as the valve opening increases and the steam flow smoothens.

The significance of this effect is that the actual cost curve function of a large steam plant is not continuous, but even more important, it is non-convex. A simple way (and the most common way) to handle these two issues is to approximate the actual curve with a smooth, convex curve, similar to the dark line of Fig. 31.

10.0 Natural gas combined cycle (NGCC) units

The following information was developed from [38, 44, 45, 46]. Fig. 32 shows US growth in NGCC power plants, by percent total energy generated, from 2002-2011 [47].

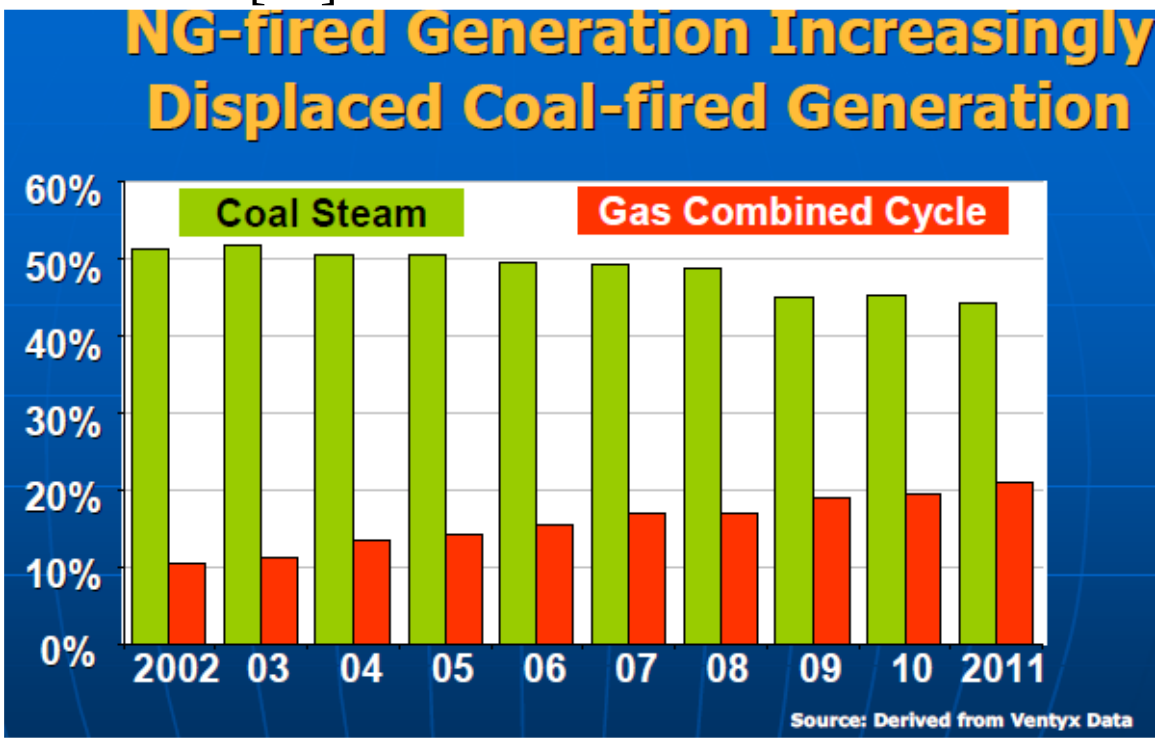

Fig. 32a: Growth in NGCC energy 2002-2011 [47]

Fig. 32b [48] shows the growth in NGCC power plants, by capacity, from 2008-2018.

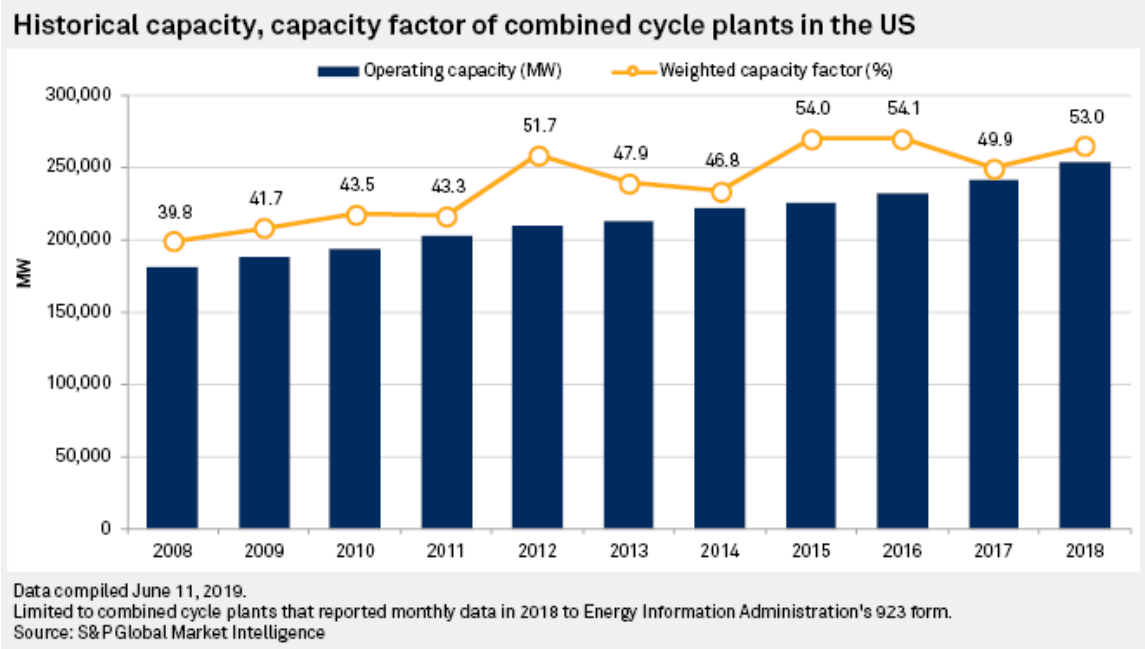

Fig. 32b: Growth in NGCC capacity 2008-2018 [48]

Fig. 32c shows the added NGCC power plants from 1990-2025 [49].

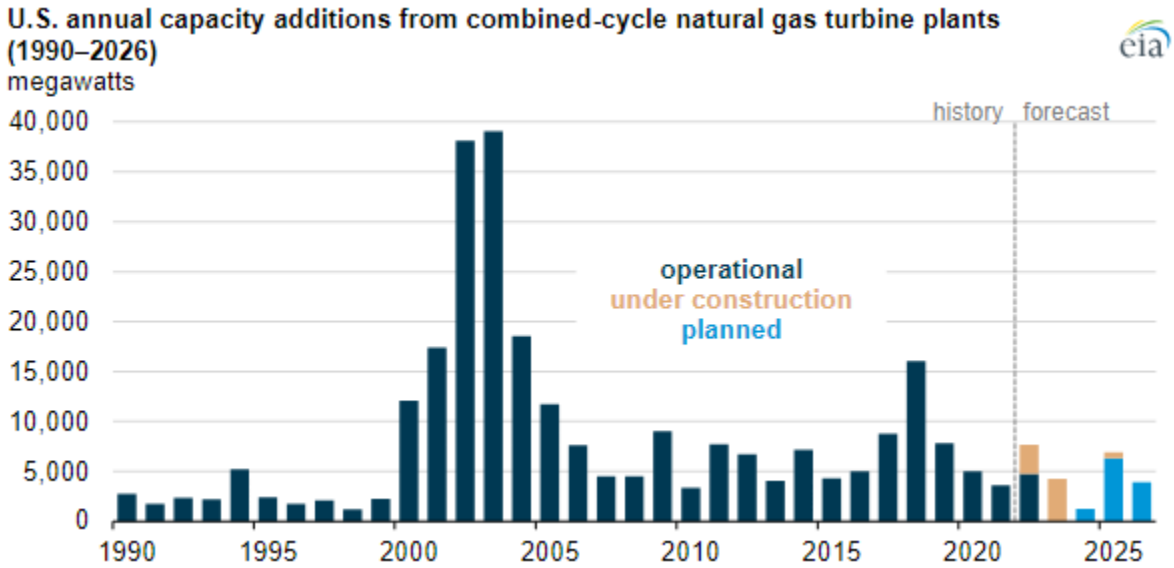

Fig. 32c: US annual capacity additions from NGCC

It is clear that NGCC plants have grown significantly over the last two decades, and based on our previous discussion, we know why: (i) shale has made gas prices low and stable; (ii) NGCC plants are more efficient than other kinds of thermal plants; (iii) gas-created CO_2 emissions from NGCC are 1/3 to 1/2 of what coal is on a MT/MWhr basis.

However, we should be aware that there is a range of efficiencies associated with NGCC plants, mainly due to the year the plant was built and therefore the technologies used in building it. Fig. 32d [50] shows how US NGCC plants have increased in efficiency (right) and correspondingly increased in capacity factor (left) since the 1990-1999 timeframe, as NGCC technology has improved.

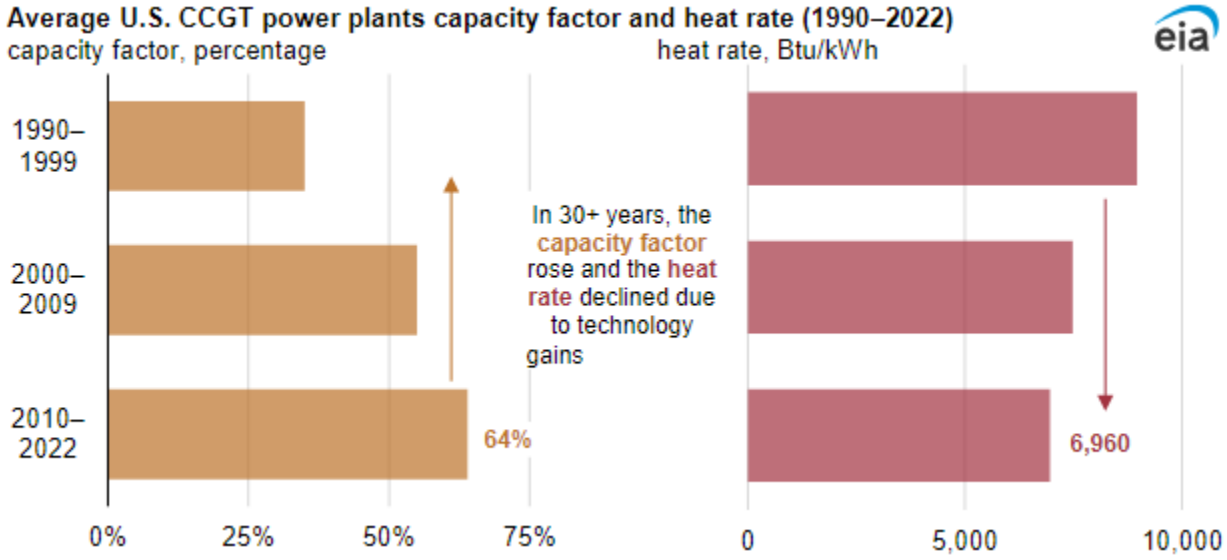

Fig. 32d, Increase in efficiency (decrease in heat rate) 1990-2022

Combined cycle units utilize both gas turbines (based on the Brayton cycle) and steam turbines (based on the Rankine cycle). Gas turbines are very similar to jet engines where fuel (can be either liquid or gas) mixed with compressed air is ignited. The combustion increases the temperature and volume of the gas flow, which when directed through a valve-controlled nozzle over turbine blades, spins the turbine which drives a synchronous generator. On the other hand, steam turbines utilize a fuel (coal, natural gas, petroleum, or uranium) to create heat which, when applied to a boiler, transforms water into high pressure superheated (above the temperature of boiling water) steam. The steam is directed through a valve-controlled nozzle over turbine blades, which spins the turbine to drive a synchronous generator.

A combined cycle power plant combines gas turbine (also called combustion turbine) generator(s) with turbine exhaust waste heat boiler(s) (also called heat recovery steam generators or HRSG) and steam turbine generator(s) for the production of electric power. The waste heat from the combustion turbine(s) is fed into the boiler(s) and steam from the boiler(s) is used to run steam turbine(s). Both the combustion turbine(s) and the steam turbine(s) produce electrical energy. Generally, the combustion

turbine(s) can be operated with or without the boiler(s).

A combustion turbine is also referred to as a simple cycle gas turbine generator. They are relatively inefficient with net heat rates at full load of some plants at 11-15 MBtu/MWhr, as compared to the 9.0 to 10.5 MBtu/MWhr heat rates typical of a large fossil fuel fired utility generating plant. This fact, combined with what can be high gas prices (especially relative to coal), make the gas turbine expensive. Yet, they can ramp up and down very quickly, so as a result, combustion turbines have mainly been used only for peaking or standby service.

The gas turbine exhausts relatively large quantities of gases at temperatures over 900 °F. In combined cycle operation, then, the exhaust gases from each gas turbine will be ducted to a waste heat boiler. The heat in these gases, ordinarily exhausted to the atmosphere, generates high pressure superheated steam. This steam will be piped to a steam turbine generator. The resulting combined cycle heat rate is in the 7.0 to 9.5 MBtu/MWhr range, significantly less than a simple cycle gas turbine generator.

In addition to the good (low) heat rates, combined cycle units have flexibility to utilize different fuels (natural gas, heavy fuel oil, low Btu gas, coal-derived gas) [51]. In fact, there were some advanced technologies under development, including the *integrated gasification combined cycle* (IGCC) plant, which makes it possible to run combined cycle on solid fuel (e.g., coal or biomass) [52]. The first two operational IGCC plants in the US were the Polk Station Plant in Tampa and the Wabash River Plant in Indiana [53]. The Ratcliffe-Kemper plant was under construction by Mississippi Power (a subsidiary of Southern Company), as 582 MW IGCC plant originally intended to be completed in 2014 [54, 55]. However, the coal gasifiers never worked properly in this plant, and today it is run only as an NGCC [56].

The flexibility of combined cycle plants, together with the fast ramp rates of the combustion turbines and relatively low heat rates, has made the combined cycle unit the unit of choice for a large percentage of recent new power plant installations. The potential, due to shale, for increased gas supply and lowered gas prices has further stimulated this tendency.

Fig. 33a shows the simplest kind of combined cycle arrangement, where there is one combustion turbine and one HRSG driving a steam turbine.

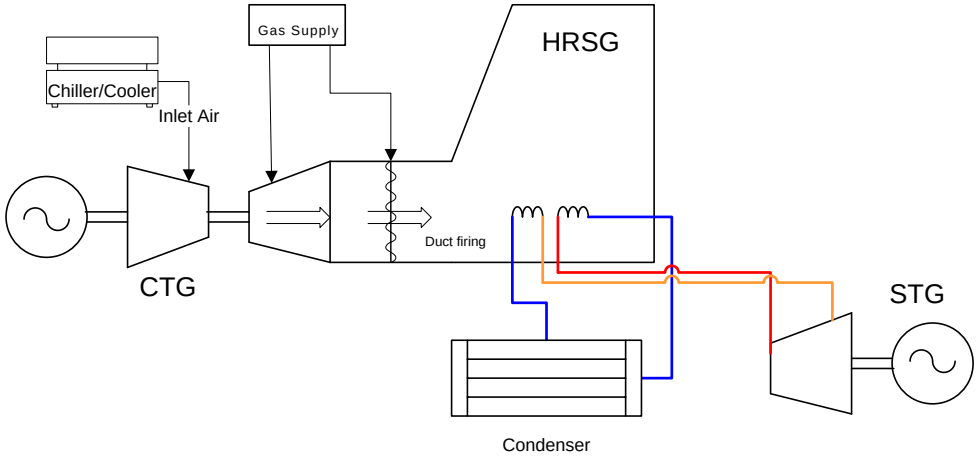

Fig. 33a: A 1 × 1 configuration

An additional level of complexity would have two combustion turbines (CT A and B) and their HRSGs driving one steam turbine generator (STG), as shown in Fig. 33b.

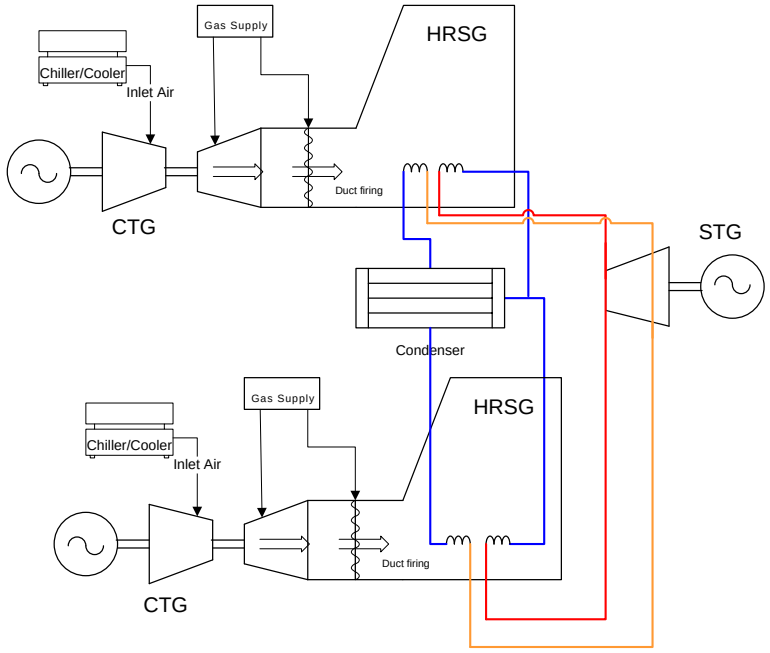

Fig. 33b: a 2 × 1 configuration

In such a design, the following six combinations are possible.

- CT A alone
- CT B alone
- CT A and CT B together
- CT A and STG
- CT B and STG
- CT A and B and STG

The modes with the STG are more efficient than the modes without the STG (since the STG utilizes CT exhaust heat that is otherwise wasted), with the last mode listed being the most efficient.

If we model a combined cycle plant as a single plant, we run into a problem. Consider the transition between the combined cycle power plant operation

just as the STG is ramped up. Previous to STG start-up, only the CT is generating, with a specified amount of fuel per hour being consumed, as a function of the CT power generation level. Then, after STG start-up, the fuel input remains almost constant, but the MW output of the (now) two generation units has increased by the amount of power produced by the steam turbine driven by the STG. A typical cost curve for this situation is shown in Fig. 34.

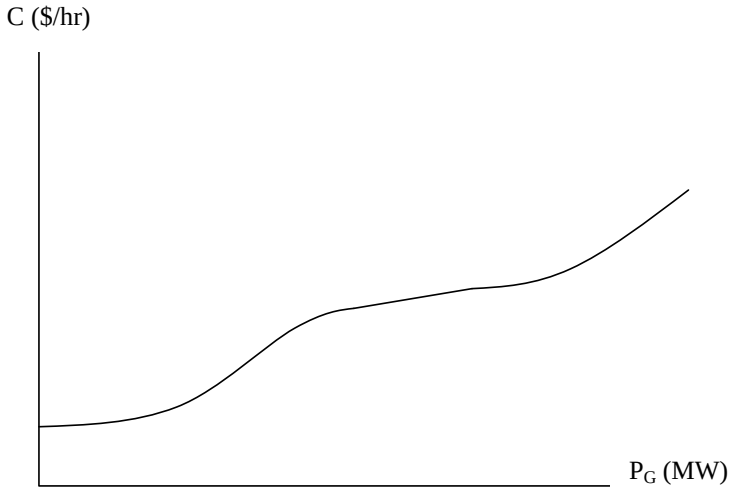

Fig. 34: Cost curve for a combined cycle plant

An important feature of the curve in Fig. 34 is that it is nonconvex, which means its slope (i.e., its incremental cost) does not monotonically increase with P_G. Figure 35 illustrates incremental cost variation with P_G.

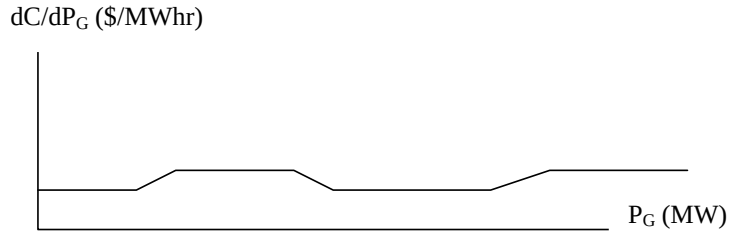

Fig. 35: Incremental cost curve for a combined cycle plant

The key attribute of the incremental cost curve, in order to satisfy convexity, is that it must be non-decreasing. Clearly, the curve of Fig. 35 does not satisfy this requirement.

11.0 Economic dispatch and convexity of objective functions in optimization

The traditional economic dispatch (ED) approach used by electric utilities for many years is very well described in [57].

This approach is still used directly by owners of multiple generation facilities when they make one offer to the market and then need to dispatch their units in the most economic fashion to deliver on this offer. This approach also provides one way to view the method by which locational marginal prices are computed in most of today's real-time market systems.

The simplest form of the ED problem is as follows:

Minimize:

$$F_T = \sum_{i=1}^{n} F_i(P_i) \tag{1}$$

Subject to:

$$\sum_{i=1}^{n} P_i = P_{load} \Longrightarrow \phi(P_i) = P_{load} - \sum_{i=1}^{N} P_i = 0 \tag{2}$$

$$\begin{aligned} P_i &\geq P_{i,\min} \Rightarrow -P_i \leq -P_{i,\min} \\ P_i &\leq P_{i,\max} \\ P_i &\geq 0 \end{aligned} \tag{3}$$

Here, we note that the equality constraint is linear in the decision variables P_i. In the Newton approach to solving this problem ([57]), we form the Lagrangian according to:

$$\mathcal{L} = F_T(P_i) + \lambda\phi(P_i) \tag{4}$$

If each and every individual cost curve $C_i(P_i)$, $i=1,n$, is quadratic, then they are all convex. Because the sum of convex functions is also a convex function, when all cost curves are convex, then the objective function $F_T(P_i)$ of the above problem is also convex. If $\phi(P_i)$ is linear, then it is convex, and therefore $\mathcal{L}$ is convex. This fact allows us to find the solution by applying *first order conditions*.

First order conditions for multi-variable calculus are precisely analogous to first order conditions to single variable calculus. In single variable calculus, we minimize $f(x)$ by solving $f'(x)=0$, on the condition that $f(x)$ is convex, or equivalently, that $f''(x)>0$.

In multivariable calculus, where $\underline{x}=[x_1\ x_2 \ldots\ x_n]^T$, we minimize $f(\underline{x})$ by solving $\underline{f'}(\underline{x})=\underline{0}$, that is,

$$\frac{\partial f}{\partial x_i}=0, \quad i=1,n \tag{5}$$

on the condition that $f(\underline{x})$ is convex or equivalently, that the Hessian matrix $\underline{f''}(\underline{x})$ is positive definite.

We recall that, in single variable calculus, if $f(x)$ is not convex, then the first order conditions do not guarantee that we find a *global* minimum. We could find a maximum, or a local minimum, or an inflection point, as illustrated in Fig. 36 below.

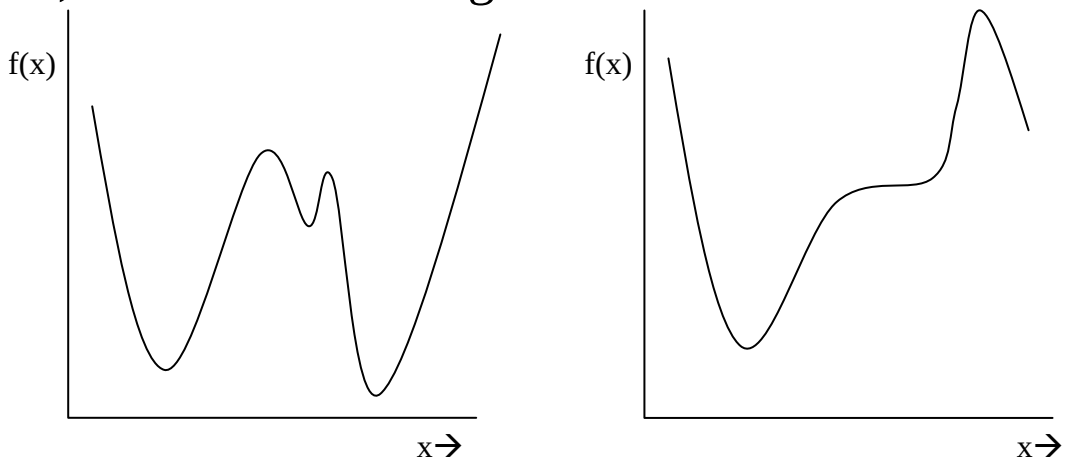

Fig. 36: Non-convex functions

The situation is the same in the multivariable case, i.e., if $f(\underline{x})$ is not convex, then the first order conditions of (5) do not guarantee a global minimum.

Now returning to the Lagrangian function of our constrained optimization problem, repeated here for convenience:

$$\mathcal{L} = F_T(P_i) + \lambda\phi(P_i) \tag{4}$$

we recall that solution to the original problem is found by minimizing F_T. But, to use what we now know, we are only guaranteed to find a global minimum of F if $\mathcal{L}$ is convex. In this case, the first order conditions results in

$$\frac{\partial \mathcal{L}}{\partial Pi} = 0, \quad i = 1, N$$

$$\frac{\partial \mathcal{L}}{\partial \lambda} = 0$$

from which we may find our solution (inequality constraints may be handled by checking the resulting solution against them, and for any violation, setting up another equality constraint which binds the given decision variable to the limit which was violated).

But if one of the units is a combined cycle unit, the F_T, and therefore $\mathcal{L}$, will not be convex. So, first order conditions do not guarantee a global minimum.

In other words, there may be a lower-cost solution than the one we will obtain from applying first order conditions. This makes engineers and managers concerned, because they worry they are spending money unnecessarily.

12.0 General solutions for non-convex optimization problems

Generation owners who utilize combined cycle units must use special techniques to solve the EDC problem. Some general methods that have been proposed for solving non-convex optimization problems are below.

1. Enumeration/Iteration: In this method, all possible solutions are enumerated and evaluated, and then the lowest cost solution is identified. This method will always work but can be quite computational.

2. Dynamic programming: See pp. 51-54 of reference [38].

3. Sequential unconstrained minimization technique (SUMT): This method is described on pp 473-477 of reference [58].

4. Heuristic optimization methods: There are a number of methods in this class, including Genetic Algorithm simulated annealing, tabu search, and particle swarm. A good reference on these methods is [59].

5. There is a matlab toolbox for handling non-convex optimization. It provides 2 different algorithms together with references on papers that describe the algorithms, located at http://tomlab.biz/. There are two methods provided:
(a) Radial Basis Function (RBF) interpolation:
(b) Efficient Global Optimization (EGO) algorithm: The idea of the EGO algorithm is to first fit a response surface to data collected by evaluating the objective function at a few points. Then, EGO balances between finding the minimum of the surface and improving the approximation by sampling where the prediction error may be high.

13.0 Practical solutions to modeling combined cycle units in optimization

Ref [60], developed by engineers at ERCOT and Ventyx (now ABB-Hitachi), is an excellent summary of practical methods to modeling combined cycle units. Ref [61] is as well. Both provide references to a number of other good

resources on the subject. The methods outlined in them are as follows:

- Aggregate modeling: Here, the combined cycle unit is simply modeled with a "best-fit" convex cost curve. This approach does not handle the non-convexity of the actual cost characteristic.
- Pseudo-unit modeling: Here, a number of pseudo-units equal to N, the number of combustion turbines are represented, each with $1/N$ of the steam unit. This works for an $N\times1$ combined cycle unit. For example, a 3×1 combined cycle unit would be modeled as three separate pseudo-units; each of the three pseudo-units would be one gas turbine plus one third of a steam turbine [62]. This approach has been implemented within several markets, including ISO NE, NYISO, MISO, PJM, and IESO. This approach does not handle the non-convexity of the actual cost characteristic.
- Configuration-based modeling: This approach is also referred to as pseudo-plant modeling. Here, a cost-curve (or incremental cost curve) is provided for each configuration of the combined cycle plant. Additional logic is provided in the security-constrained unit commitment (SCUC, which is the mixed integer programming software for the day-ahead market) to ensure that only one configuration can be selected, and that the selection depends on the configuration of the previous time period, as illustrated in Fig. 37 below for a 2×1 combined cycle plant [60]. The configuration chosen by SCUC for any one hour is maintained for the entire hour in the real-time market. CAISO has implemented this approach, it is well-described in [62].

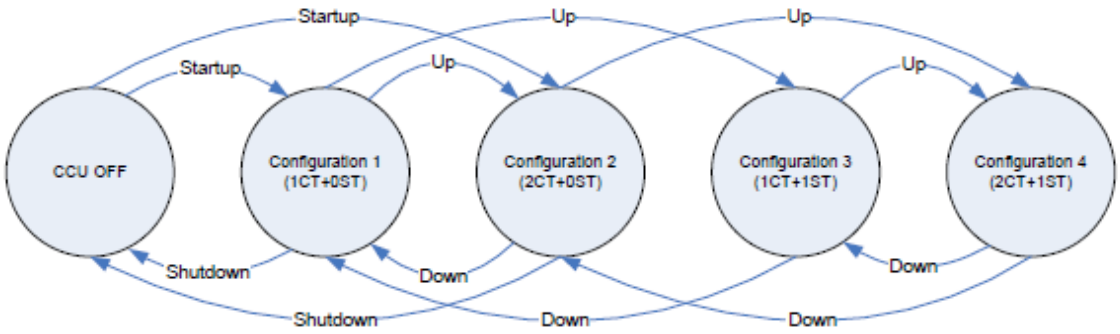

Fig. 37

- Physical-unit modeling: Here, each CT and STG is considered to be an individual resource with its own individual offers. This is a bad market model but it provides good fidelity in terms of MW that the power plant can actually produce. ERCOT reports in [62] that it utilizes configuration-based models for its markets and physical unit modeling for its network security applications.

Of the various above-described approaches, most market operators use either the aggregate modeling approach or the configuration-based approach [61].

References

[1] J. McCalley, W. Jewell, T. Mount, D. Osborn, and J. Fleeman, "A wider horizon: Technologies, Tools, and Procedures for Energy System Planning at the National Level," IEEE Power and Energy Magazine, May/June, 2011.

[2] J. Morgan, "Energy Density and Waste Comparison of Energy Production," Nuclear Science and Technology, June 2010, available at http://nuclearfissionary.com/2010/06/09/energy-density-and-waste-comparison-of-energy-production.

[3] The World Nuclear Association, "The Economics of Nuclear Power," 2010, available at http://www.world-nuclear.org/info/inf02.html.

[4] World Nuclear Association, "Economics of Nuclear Power," Updated March 2020, available at https://www.world-nuclear.org/information-library/economic-aspects/economics-of-nuclear-power.aspx.

[5] US Energy Information Administration, "Uranium Marketing Annual Report," May 26, 2020, https://www.eia.gov/uranium/marketing/.

[6] https://www.eia.gov/electricity/annual/#seven

[7] US Energy Information Administration, "Table 7.1. Receipts, Average Cost, and Quality of Fossil Fuels for the Electric Power Industry, 2012 through 2022." Available: www.eia.gov/electricity/annual/html/epa_07_01.html.

[8] U.S. Department of Energy, Energy Information Administration website, located at http://www.eia.doe.gov/emeu/aer/txt/ptb0811b.html.

[9] US Energy Information Administration, "Natural Gas Explained," Accessed 2/3/2024. Available:

www.eia.gov/energyexplained/natural-gas/use-of-natural-gas.php.
[10] US Energy Information Administration, "Electricity Energy Infrastructure and Resources." Accessed 2/3/2024. Available: https://atlas.eia.gov/apps/895faaf79d744f2ab3b72f8bd5778e68/explore.
[11] P. Zummo, "America's Electricity Generation Capacity, 2020 Update," American Public Power Association, March, 2020, www.publicpower.org/system/files/documents/Americas-Electricity-Generation-Capacity-2020.pdf.
[12] Statista, "Share of electricity capacity additions in the United States from 2010 to 2022, by source." Accessed 2/3/2024. Available: www.statista.com/statistics/525735/share-of-us-electricity-capacity-additions-by-resource/.
[13] North American Reliability Corporation (NERC), "2020 Long Term Reliability Assessment," Dec., 2020, www.nerc.com/pa/RAPA/ra/Reliability%20Assessments%20DL/NERC_LTRA_2020_Errata.pdf.
[14] National Electric Reliability Corporation (NERC), "2023 Long-Term Reliability Assessment," Dec. 2023. Accessed 2/3/2024. Available: www.nerc.com/pa/RAPA/ra/Reliability%20Assessments%20DL/NERC_LTRA_2023.pdf.
[15] EIA Energy Mapping System, www.eia.gov/state/maps.php?v=Coal.
[16] https://upload.wikimedia.org/wikipedia/commons/0/04/U.S._annual_coal_production_by_basin%2C_2014-2018_%2831930259427%29.png
[17] http://www.rggi.org/.
[18] Regional Greenhouse Gas Initiative (RGGI), "How RGGI Works." Accessed 2/3/2024. Available: www.rggi.org/sites/default/files/Uploads/Fact%20Sheets/RGGI_Intro_Factsheet.pdf.
[19] Wikipedia page on "Greenhouse gas": http://en.wikipedia.org/wiki/Carbon_emissions
[20] US Department of Energy, Energy Information Administration, "Emissions of Greenhouse Gases in the United States 2006," November 2007.
[21] US Department of Energy, Energy Information Administration, "Emissions of Greenhouse Gases in the United States 2008," December 2009.
[22] https://flowcharts.llnl.gov/commodities/carbon
[23] https://www.eia.gov/todayinenergy/detail.php?id=34192
[24] https://www.eia.gov/environment/emissions/carbon/
[25] https://www.eia.gov/todayinenergy/detail.php?id=37392
[26] US Energy Information Administration (EIA), "U.S. Energy-Related Carbon Dioxide Emissions, 2022." Accessed 2/5/2024. Available: www.eia.gov/environment/emissions/carbon/#:~:text=Changes%20in%20electricity%20generation%20sources,2%20per%20GWh%20in%202022.
[27] F. Van Aart, "Energy efficiency in power plants," October 21, 2010, Vienna, available from Dr. McCalley (see "New Generation" folder), but you must make request.
[28] EPA report, www.epa.gov/airmarkt/progsregs/epa-ipm/docs/chapter8-v2_1-update.pdf.
[29] Black & Veatch, "Planning for Growing Electric Generation Demands," slides from a presentation to Kansas Energy Council – Electric Subcommittee, March 12, 2008, available at http://www.google.com/search?hl=en&source=hp&q=%22Planning+for+Growing+Electric+Generation+Demands%22&btnG=Google+Search&aq=f&aqi=&aql=&oq=&gs_rfai=C5Ekv4uV7TP7ECIzmNJHV_MIEAAAAqgQFT9Dr5Lw.
[30] DOE EIA Website for US locations emission coefficients, http://www.eia.doe.gov/oiaf/1605/ee-factors.html.
[31] Iowa Renewable Energy, Blog, Accessed 2/5/2024. Available: https://blog.arcadia.com/iowa-renewable-energy/.
[32] Iowa Environmental Council, "IEC's 2021 Condition of the State: The True Cost of Coal-Fired Power Generation in Iowa," Sept. 8, 2021. Accessed 2/5/2024. Available: https://www.iaenvironment.org/newsroom/energy-news/iec-2021-condition-of-the-state.
[33] Iowa Utilities Board, Accessed Feb. 6, 2024. Available: https://iub.iowa.gov/regulated-industries/electric/iowas-electric-profile.
[34] www.rutlandherald.com/apps/pbcs.dll/article?AID=/20080706/NEWS04/807060457/1024/NEWS04
[35] A. Wood and B. Wollenberg, "Power Generation, Operation, and Control," second edition, Wiley-Interscience, 1996.
[36]H. Stoll, "Least-cost electric utility planning," 1989, John Wiley.
[37] D. Kirschen and G. Strbac, "Fundamentals of Power System Economics," Wiley, 2004.
[38] A. J. Wood and B. F. Wollenberg, Power, Generation, Operation and Control, second edition, John Wiley & Sons, New York, NY, 1996.

[39] J. Klein, "The Use of Heat Rates in Production Cost Modeling and Market Modeling," California Energy Commission Report, 1998.
[40] The great Texas freeze: February 11-20, 2021. Available: www.ncei.noaa.gov/news/great-texas-freeze-february-2021.
[41] S. Patel, "ERCOT Sheds Load as Extreme Cold Forces Generators Offline; MISO, SPP Brace for Worsening System Conditions," Power, Feb 15, 2021, www.powermag.com/ercot-sheds-load-as-extreme-cold-forces-generators-offline-miso-spp-brace-for-worsening-system-conditions/.
[42] L. Tesfatsion, "Auction Basics for Wholesale Power Markets: Objectives and Pricing Rules," Proceedings of the 2009 IEEE Power and Energy Society General Meeting, July, 2009.
[43] J. Kim, D. Shin, J. Park, and C. Singh, "Atavistic genetic algorithm for economic dispatch with valve point effect," Electric Power Systems Research, 62, 2002, pp. 201-207.
[44] "Electric power plant design," chapter 8, publication number TM 5-811-6, Office of the Chief of Engineers, United States Army, January 20, 1984, located at http://www.usace.army.mil/publications/armytm/tm5-811-6/, not under copyright.
[45] A. Cohen and G. Ostrowski, "Scheduling units with multiple operating modes in unit commitment," IEEE ???, 1995.
[46] A. Birch, M. Smith, and C. Ozveren, "Scheduling CCGTs in the Electricity Pool," in "Opportunities and Advances in International Power Generation, March 1996.
[47] 2011 State of the Markets, a FERC presentation, April 2012, at https://www.ferc.gov/market-oversight/reports-analyses/st-mkt-ovr/som-rpt-2011.pdf.
[48] S. Tsao and H. Javier, "1 in 7 new combined-cycle plants are little-used, analysis finds,"S&P Global, July 29, 2019, www.spglobal.com/marketintelligence/en/news-insights/trending/Pu5fAcJoqopojxYhGN0tMw2.
[49] US Energy Information Administration, "U.S. electric-generating capacity for combined-cycle natural gas turbines is growing," Nov. 4, 2022. Available: www.eia.gov/todayinenergy/detail.php?id=54539.
[50] US Energy Information Administration, "Natural gas combined-cycle power plants increased utilization with improved technology," Nov. 20, 2023. Available: www.eia.gov/todayinenergy/detail.php?id=60984#:~:text=The%20average%20utilization%20rate%20(or,2008%20to%2057%25%20in%202022.
[51] R. Tawney, K. Kamali, W. Yeager, "Impact of different fuels on reheat and nonreheat combined cycle plant performance," Proceedings of the American Power Conference; Vol/Issue: 50; American power conference; 18-20 Apr 1988; Chicago, IL (USA).
[52] I. Burdon, "Winning combination [integrated gasification combined-cycle process]," IEE Review, Volume: 52 , Issue: 2, 2006 , pp. 32 – 36, IET Journals & Magazines.
[53] www.fossil.energy.gov/programs/powersystems/gasification/gasificationpioneer.html
[54] "Southern Company on track with new generation," Investopedia, March 23, 2011, available at http://www.investopedia.com/stock-analysis/2011/southern-company-on-track-with-new-generation-so-d-duk0323.aspx#axzz28iY0dqaR.
[55] www.southerncompany.com/smart_energy/smart_power_vogtle-kemper.html
[56] S; Wilson, "Two years since Kemper clean coal project ended," Mississippi Center for Public Policy, July, 2019, https://mspolicy.org/two-years-since-kemper-clean-coal-project-ended/.
[57] G. Sheble and J. McCalley, "Module E3: Economic dispatch calculation," used in EE 303 at Iowa State University.
[58] F. Hillier and G. Lieberman, "Introduction to Operations Research," fourth edition, Holden-Day, 1986.
[59] "Tutorial on modern Heuristic Optimization Techniques with Applications to Power Systems," IEEE PES Special Publication 02TP160, edited by K. Lee and M. El-Sharkawi, 2002.
[60] H. Hui, C. Yu, F. Gao, and R. Surendran, "Combined cycle resource scheduling in ERCOT nodal market," Proc. of the 2011 IEEE PES General Meeting, 2011.
[61] C. Dai, Y. Chen, F. Wang, J. Wan, and L. Wu, "A configuration-component-based hybrid model for combined cycle units in MISO day-ahead market," IEEE Trans on Power Systems, Vol. 34, No. 2, March 2019.
[62]"Modeling of Multi-Stage Generating Units," CAISO. Available at www.caiso.com/2358/2358e27f11070.pdf.